

UNCLASSIFIED

| |
|--|
| |
| |
| |
| |
| AD NUMBER |
| AD467839 |
| NEW LIMITATION CHANGE |
| TO Approved for public release, distribution unlimited |
| FROM Distribution authorized to U.S. Gov't. agencies and their contractors; Administrative/Operational Use; Jun 1965. Other requests shall be referred to Air Force Materials Lab., Wright-Patterson AFB, OH 45433. |
| AUTHORITY |
| AFSC/IST [WPAFB, OH] ltr dtd 21 Mar 1989 |

THIS PAGE IS UNCLASSIFIED

AFML-TR-65-2-
Part IV, Vol I

TERNARY PHASE EQUILIBRIA
IN TRANSITION METAL-BORON-CARBON-SILICON SYSTEMS

Part IV. Thermochemical Calculations

Volume I. Thermodynamic Properties
of Group IV, V, and VI Binary Transition Metal Carbides

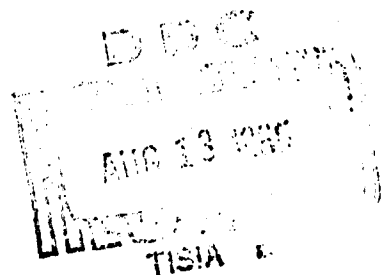
Y.A. Chang

Aerojet-General Corporation

TECHNICAL REPORT NO. AFML-TR-65-2, Part IV, Volume I

June 1965

Air Force Materials Laboratory
Research and Technology Division
Air Force Systems Command
Wright-Patterson Air Force Base, Ohio



25264

see form
11/15/65

AD 462839

AD 462839

SECURITY

MARKING

The classified or limited status of this report applies to each page, unless otherwise marked.

Separate page printouts MUST be marked accordingly.

THIS DOCUMENT CONTAINS INFORMATION AFFECTING THE NATIONAL DEFENSE OF THE UNITED STATES WITHIN THE MEANING OF THE ESPIONAGE LAWS, TITLE 18, U.S.C., SECTIONS 793 AND 794. THE TRANSMISSION OR THE REVELATION OF ITS CONTENTS IN ANY MANNER TO AN UNAUTHORIZED PERSON IS PROHIBITED BY LAW.

NOTICE: When government or other drawings, specifications or other data are used for any purpose other than in connection with a definitely related government procurement operation, the U. S. Government thereby incurs no responsibility, nor any obligation whatsoever; and the fact that the Government may have formulated, furnished, or in any way supplied the said drawings, specifications, or other data is not to be regarded by implication or otherwise as in any manner licensing the holder or any other person or corporation, or conveying any rights or permission to manufacture, use or sell any patented invention that may in any way be related thereto.

NOTICES

When Government drawings, specifications, or other data are used for any purpose other than in connection with a definitely related Government procurement operation, the United States Government thereby incurs no responsibility nor any obligation whatsoever; and the fact that the Government may have formulated, furnished, or in any way supplied the said drawings, specifications, or other data, is not to be regarded by implication or otherwise as in any manner licensing the holder or any other person or corporation, or conveying any rights or permission to manufacture, use, or sell any patented invention that may in any way be related thereto.

Qualified users may obtain copies of this report from the Defense Documentation Center. The distribution of this report is limited because it contains technology identifiable with items on the Mutual Defense Assistance Control List excluded from export under U.S. Export Control Act of 1949, as implemented by AFR 400-10.

Copies of this report should not be returned to the Research and Technology Division unless return is required by security considerations, contractual obligations, or notice on a specific document.

I
I



AEROJET-GENERAL CORPORATION

SACRAMENTO

CALIFORNIA

SACRAMENTO PLANT

2443:65-066:pjb
22 July 1965


Subject: Report AFML-TR-65-2
Part IV, Volume I
Ternary Phase Equilibria in
Transition Metal-Boron-Carbon-
Silicon Systems

To: Air Force Materials Laboratory
Research & Technology Division
Wright-Patterson Air Force Base, Ohio

Attn: Capt. R. A. Peterson

Inclosure (1) is submitted in partial fulfillment of Contract AF 33(615)-1249.

AEROJET-GENERAL CORPORATION


R. L. Fulford, Supervisor
Editorial Services
Technical Publications

Incl: (1) Copies 1 through 18, Report AFML-TR-65-2
Part IV, Volume I

TERNARY PHASE EQUILIBRIA
IN TRANSITION METAL-BORON-CARBON-SILICON SYSTEMS

Part IV. Thermochemical Calculations
Volume I. Thermodynamic Properties of
Group IV, V, and VI Binary Transition Metal Carbides

Y. A. Chang

FOREWORD

This report was prepared by the Materials Research Laboratory, Aerojet-General Corporation, Sacramento, California under USAF Contract No. AF 33(615)-1249. The contract was initiated under Project No. 7350, "Refractory, Inorganic Non-Metallic Materials", Task No. 735001, "Non-Graphitic". The work was administered under the direction of the Air Force Materials Laboratory, Research and Technology Division, with Captain R. A. Peterson acting as Project Engineer, and Dr. E. Rudy, Aerojet-General Corporation, as Principal Investigator.

The author is indebted to Dr. Rudy for his guidance and many fruitful discussions. He also wishes to thank Messrs. L. Nole and J. Howard of the Computing Sciences Division who prepared the various computer programs used in this compilation; Dr. A.J. Stosick, Senior Scientist, who made many helpful suggestions; and Prof. Dr.H. Nowotny, University of Vienna, who served as consultant to the project.

The manuscript of this report was released by the author May 1965 for publication as an RTD Technical Report.

Other reports issued under USAF Contract AF 33(615)-1249 have included:

Part I, Related Binaries

Volume I, Mo-C System

Volume II, Ti-C and Zr-C System

Part III, Special Experimental Techniques

Volume I, High Temperature Differential Thermoanalysis

FOREWORD (Cont'd)

This technical report has been reviewed and is approved.

A handwritten signature in black ink, appearing to read 'W. G. Ramke', written in a cursive style.

W. G. RAMKE
Chief, Ceramics and Graphite Branch
Metals and Ceramics Division
Air Force Materials Laboratory

ABSTRACT

All available data concerning the thermodynamic properties of the group IV, V, and VI binary metal carbides have been critically evaluated and the values judged to be most reliable were selected. The compositional variation of the free energies of the group IV binary metal carbides has been calculated based on theoretical models.

TABLE OF CONTENTS

| | PAGE |
|--|------|
| I. <u>INTRODUCTION & SUMMARY</u> | 1 |
| A. Introduction | 1 |
| B. Summary | 2 |
| II. <u>EVALUATION OF THE THERMODYNAMIC PROPERTIES</u> <u>OF BINARY CARBIDES</u> | 2 |
| A. Method of Evaluation | 2 |
| 1. Phase Diagram | 3 |
| 2. Low-Temperature Data | 4 |
| 3. High-Temperature Data | 5 |
| 4. Reaction Equilibrium Data | 7 |
| 5. Vapor Pressure Data | 8 |
| 6. Calorimetric Data | 9 |
| 7. Selection of Enthalpy and Free Energy Data | 9 |
| B. Experimental Thermodynamic Properties of Binary Carbides | 10 |
| 1. Group IV Metal and Metal Carbon Systems | 10 |
| a. Titanium-Carbon System | 10 |
| b. Zirconium-Carbon System | 17 |
| c. Hafnium | 24 |
| d. Hafnium-Carbon System | 28 |
| 2. Group V Metal Carbon Systems | 34 |
| a. Vanadium-Carbon System | 34 |
| b. Niobium-Carbon System | 40 |
| c. Tantalum-Carbon System | 47 |

| TABLE OF CONTENTS (continued) | | PAGE |
|-------------------------------|--|------|
| 3. | Group VI Metal Carbon Systems | 55 |
| a. | Chromium-Carbon System. | 55 |
| b. | Molybdenum-Carbon System. | 64 |
| c. | Tungsten-Carbon System. | 67 |
| III. | <u>CALCULATION OF THERMODYNAMIC PROPERTIES</u> <u>OF NON-STOICHIOMETRIC BINARY CARBIDES</u> | 73 |
| A. | Theoretical Models | 74 |
| 1. | Interstitial Model as Applied to the Terminal Solid Solution | 74 |
| 2. | Schottky-Wagner Vacancy Model | 77 |
| B. | Calculated Thermodynamic Properties of Binary Carbides | 86 |
| 1. | Hafnium-Carbon System. | 86 |
| 2. | Zirconium-Carbon and Titanium-Carbon Systems | 89 |
| 3. | Discussion | 93 |
| | References. | 99 |

| FIGURE | ILLUSTRATIONS | PAGE |
|--------|--|------|
| 1 | The Phase Diagram of the Titanium-Carbon System | 11 |
| 2 | The Phase Diagram of the Zirconium-Carbon System | 18 |
| 3 | The Phase Diagram of the Hafnium-Carbon System | 28 |
| 4 | The Phase Diagram of the Vanadium-Carbon System | 35 |
| 5 | The Phase Diagram of the Niobium-Carbon System | 40 |
| 6 | The Heats of Formation of the Niobium Monocarbide and the Subcarbide | 46 |
| 7. | The Phase Diagram of the Tantalum-Carbon System | 48 |
| 8 | The Heats of Formation of the Tantalum Monocarbide and the Subcarbide | 53 |
| 9 | The Phase Diagram of the Chromium-Carbon System | 56 |
| 10 | The Phase Diagram of the Molybdenum-Carbon System | 65 |
| 11 | The Phase Diagram of the Tungsten-Carbon System | 68 |
| 12a | Gibbs Free Energies of Formation of the α -, β -, and | 90 |
| 12b | γ -phases in the Hafnium-Carbon System | 91 |
| 13 | The Partial Molar Free Energies of Hafnium and Carbon | 92 |
| 14 | Gibbs Free Energy of Formation of the γ -phase in the Zirconium-Carbon System | 94 |
| 15 | The Partial Molar Free Energies of Zirconium and Carbon | 95 |
| 16 | Gibbs Free Energy of Formation of the γ -phase in the Titanium-Carbon System | 96 |
| 17 | The Partial Molar Free Energies of Titanium and Carbon | 97 |

TABLES

| TABLE | | PAGE |
|-------|--|------|
| 1 | High-Temperature Thermal Properties of Hafnium | 26 |
| 2 | High-Temperature Thermal Properties of Hafnium-Carbide | 31 |
| 3 | High-Temperature Thermal Properties of $\text{VC}_{0.87}$ | 37 |
| 4 | High-Temperature Thermal Properties of $\text{NbC}_{\sim 1.0}$ | 43 |
| 5 | High-Temperature Thermal Properties of $\text{TaC}_{\sim 1.0}$ | 50 |
| 6 | High-Temperature Thermal Properties of $\text{CrC}_{2/3}$ | 58 |
| 7 | High-Temperature Thermal Properties of $\text{CrC}_{3/7}$ | 58 |
| 8 | High-Temperature Thermal Properties of $\text{CrC}_{6/23}$ | 59 |
| 9 | High-Temperature Thermal Properties of $\text{WC}_{0.99}$ | 71 |

SYMBOLS

| | |
|--------------------------|---|
| P | Pressure, commonly vapor pressure . |
| V | Volume. |
| T | Absolute temperature in °K. |
| S | Entropy . |
| H | Enthalpy or heat content. |
| G | Gibbs free energy, $G = H - TS$. |
| C_p | Heat capacity at constant pressure. |
| T_{st} | Standard temperature, 298.15°K, to which many properties are referred. |
| $H_T - H_{st}$ | Enthalpy (heat content) of a substance at temperature T relative to its enthalpy at 298.15°K. |
| $S_T - S_{st}$ | Entropy of a substance at a temperature T relative to its entropy at 298.15°K. |
| $\frac{G_T - H_{st}}{T}$ | The free energy function . |
| fe_f | Abbreviation for the free energy function. |
| ΔH_f | The enthalpy (heat), Gibbs free energy, and entropy of formation of a substance from the component elements in their stable forms at the temperature and one atmosphere pressure. |
| ΔG_f | |
| ΔS_f | |
| ΔH_v | Enthalpy (heat) of vaporization. |
| ΔH_R | Enthalpy (heat) of reaction . |
| $\Delta H^{a-\beta}$ | The enthalpy (heat), Gibbs free energy, and entropy of transformation from one crystal structure α to a second crystal structure, β . |
| $\Delta G^{a-\beta}$ | |
| $\Delta S^{a-\beta}$ | |

Symbols (continued)

| | |
|--|--|
| $\Delta H^{\beta \rightarrow L}$ $\Delta G^{\beta \rightarrow L}$ $\Delta S^{\beta \rightarrow L}$ | The enthalpy (heat), Gibbs free energy, and entropy of melting from a crystalline structure β to liquid. |
| $\overline{\Delta H}_i$ $\overline{\Delta G}_i$ $\overline{\Delta S}_i$ | The partial molar enthalpy (heat), free energy, and entropy of component i in an alloy referred to its standard state. |
| $\Delta G_{f, x_o}^*$ | Free energy of formation of an ordered alloy at the stoichiometric composition |
| G_{Me^+} | Free energy of creating a metal vacancy on the metal sublattice. |
| G_{C^+} | Free energy of creating a carbon vacancy on the carbon sublattice. |
| S_{mix} | Entropy of mixing |
| ΔC_p | Deviation from Kopp's law of additivity. |
| B | A constant in the α -Hf terminal solid solution. |
| Me | Transition metal |
| N | Avogadro number |
| N_i | Number of interstitial sites in a crystal |
| N_s | Total number of lattice sites in a crystal |
| N_{Me^+} | Number of vacant metal sites |
| N_{C^+} | Number of vacant carbon sites |
| R | Universal gas constant, kN |
| Y | Average heat capacity, $\frac{H_T - H_{st}}{T - 298.15}$ |
| W | Thermodynamic Probability |

Symbols (continued)

| | |
|--------------------------------------|--|
| a | A vacancy parameter |
| a, b, c, d a', b', d' | Coefficients used in the empirical Kelley equation. |
| n_{Me+} | Number of vacant metal sites divided by the Avogadro number. |
| n_{C+} | Number of vacant carbon sites divided by the Avogadro number. |
| x | Composition of carbon component in the alloy |
| y | Number of lattice sites divided by the Avogadro number |
| x_0 | The stoichiometric composition |
| $x_{\alpha\gamma}$ | The phase boundary of α -phase in the $\alpha+\gamma$ two-phase field |
| $x_{\gamma\alpha}$ | The phase boundary of γ -phase in the $\alpha+\gamma$ two-phase field |
| $x_{\alpha\beta}$ | The phase boundary of α -phase in the $\alpha+\beta$ two-phase field |
| $x_{\beta\alpha}$ | The phase boundary of β -phase in the $\alpha+\beta$ two-phase field |
| $c, l, gr, <ss>$ | Refer to the crystalline, liquid, and gas state; graphite; and solid solution |
| $\alpha, \beta, \gamma, \text{etc.}$ | Designation for the polymorphic phases of a substance and the various phases existing in an alloy system |
| λ_1 λ_2 | The undetermined Lagrange multipliers |
| ϕ_1 ϕ_2 | Mathematical function |
| \ln | Natural logarithm, i.e. to the base e |

I. INTRODUCTION AND SUMMARY

A INTRODUCTION

The primary aim of a chemical thermodynamicist is to be able to predict the extent to which a substance will undergo reactions with other materials or will decompose into other materials. Unfortunately, the capability of making such predictions is often hampered by the lack of pertinent thermodynamic data or because of inconsistent data existing in the literature. The primary object of the present report is to evaluate the available thermodynamic properties of the group IV, V, and VI transition metal carbides based on the known thermodynamic relations and to select self-consistent data for all these carbides.

Since the transition metal carbides, like many other inorganic compounds, exist over a wide range of homogeneity, it is necessary to know the activities or the partial molar free energies of the metal and carbon components in these carbide phases as a function of composition in order to predict the stability of the carbide phases under different environments. However, most of the thermodynamic data reported in the literature are restricted to or are close to the stoichiometric composition. To extend the useful range of these data, the compositional variation of the partial molar free energies of the metal and carbon components present in the alloy phases has been calculated using the Schottky-Wagner vacancy model for all the monocarbide phases, and an interstitial model for the terminal solid solution in the second part of the report. In this interstitial model, it is assumed that the thermal free energy of the solid solution is proportional to the concentration of carbon and the configurational free energy is entirely due to

the entropy of mixing of the interstitial carbon atoms among the available interstitial sites.

B. SUMMARY

All available data concerning the thermodynamic properties of the elemental hafnium and the group IV, V, and VI transition metal carbides have been critically evaluated and the values judged to be most reliable were selected. For the group IV transition metal monocarbide phases, the integral and partial molar free energies of the metal and carbon components were calculated as a function of composition using the Schottky-Wagner vacancy model. The three Schottky-Wagner parameters which were needed to calculate the compositional variation of the free energy were obtained from the known phase relationships and from the integral free energy of formation of the monocarbide phase at the stoichiometric composition. For the α -Hf terminal solid solution, whose range of homogeneity — in contrast to the behavior of the terminal solid solutions of titanium and zirconium — is large at high temperature, the variation of the free energy with composition was calculated using the interstitial model.

II. EVALUATION OF THE THERMODYNAMIC PROPERTIES OF BINARY CARBIDES

A. METHOD OF EVALUATION

The available thermodynamic data of the group IV, V, and VI transition-metal carbides have been evaluated for self-consistency based on the known thermodynamic relations. Moreover, the validity of the thermodynamic data were also judged in the light of the experimental methods used, the uncertainties in the experimental results, the purity of the specimen, and the agreement between the values reported by the different

investigators using either the same or different experimental techniques. Since many of the binary carbide phases exist over a wide range of homogeneity, a knowledge of the exact chemical compositions is necessary in order to obtain meaningful data.

Frequently when two sets of conflicting data were reported in the literature, we have selected the results of the investigators who have previously reported reliable data for other carbides using the same experimental method.

The discussion of the data evaluation was divided into six sections: Phase Diagram, Low-Temperature Data, High-Temperature Data, Reaction Equilibrium Data, Vapor Pressure Data, and Calorimetric Data. Based on the discussion and evaluation of the reported thermodynamic data, enthalpy and free energy data were selected.

1. Phase Diagram

Phase diagrams provide much thermodynamic information. For instance at any temperature in a two phase field, the partial molar free energies of the component elements at the respective phase boundaries are equal. For the group IV metal monocarbide phases, the three Schottky-Wagner parameters have been obtained using the information that the partial molar free energy of carbon at the carbon-rich phase boundary of the monocarbide phase is the same as that of pure graphite, and the partial molar free energy of metal at the metal-rich phase boundary is equal to that in the terminal metal solid solution.

The phase diagrams of the nine binary metal carbon systems used in this compilation were taken either from those recently

established by Rudy⁽²⁾ and co-workers of our own laboratory or those already existing in the literature.

2. Low-Temperature Data

One of the thermodynamic quantities needed to describe the stability of a substance is entropy. The standard entropy of solids at 298.15°K may be obtained from the low temperature heat capacity using the following thermodynamic equation:

$$S_{st} = S_{0\cdot K} + \int_0^{298.15} \frac{C_p dT}{T}$$

where S stands for the entropy, C_p is the heat capacity at constant pressure, and T is the absolute temperature. The subscript st stands for the standard temperature, 298.15°K. The term $S_{0\cdot K}$ is zero for an ordered phase and has a positive value for a disordered phase. For a carbide phase with the stoichiometric composition such as TaC, the value of $S_{0\cdot K}$ will be zero.

The low-temperature heat capacity may be determined from some temperature close to absolute zero, usually the liquid helium, liquid hydrogen, or liquid nitrogen temperature, up to about room temperature. The heat capacity in the temperature range from absolute zero up to the lowest temperature at which a measurement is made can be calculated from theory.

In this compilation, only the values of S_{st} and $\Delta S_{f, st}$ where $\Delta S_{f, st}$ is the entropy of formation of a carbide phase at 298.15°K, all expressed in cal/deg g-atom metal are reported.

3. High-Temperature Data

The high-temperature heat content data determined calorimetrically were evaluated using the Y-function which is defined as:

$$Y = \frac{H_T - H_{st}}{T - 298.15}$$

where $(H_T - H_{st})$ is the heat content at any temperature T relative to the heat content at 298.15°K. At 298.15°K, $Y = C_p$ and $\frac{dC_p}{dT} = 2 \frac{dY}{dT}$.

In evaluating the high-temperature heat content data, the values of Y and $\frac{dY}{dT}$ at 298.15°K were made to be consistent with the values of C_p and $\frac{dC_p}{dT}$.

Once the values of Y as a function of temperature were selected, the values of heat capacity, heat content, entropy content, and free energy function were calculated by means of the following equations:

$$C_p = Y + \frac{dY}{dT} (T - 298.15)$$

$$H_T - H_{st} = Y (T - 298.15)$$

$$S_T - S_{st} = Y \left(1 - \frac{298.15}{T}\right) + \int_{298.15}^T \frac{Y(T-298.15)}{T^2} dT$$

$$-\frac{G_T - H_{st}}{T} = -\frac{Y(T-298.15)}{T} + S_T$$

where $-\frac{G_T - H_{st}}{T}$ is called the free energy function and will be abbreviated by the symbol f_{ef} in this compilation. The standard entropy required to obtain the free energy function as shown in the last equation is derived from the low-temperature heat capacity data.

The numerical calculation of C_p , $H_T - H_{st}$, $S_T - S_{st}$, and $-\frac{G_T - H_{st}}{T}$ was carried out by an IBM-7094 computer. The integral, $\int_{298.15}^T \frac{Y(T-298.15)}{T^2} dT$, was approximated with Simpson's rule. The performance of the computer program was checked using the thermal data of titanium and of iron selected by Hultgren, Orr, Anderson, and Kelley⁽¹⁾. The agreement of the values of $S_T - S_{st}$ and of $-\frac{G_T - H_{st}}{T}$ at any temperature (including the temperatures where transformations occur) between the computer-calculated values and those selected by Hultgren, et.al. was within 0.01 cal/deg g-atom. The computer-calculated C_p values were plotted as a function of temperature and the smoothed values which are consistent with the calculated heat content values were tabulated.

The heat contents of these binary carbides are represented by the following empirical Kelley equation:

$$H_T - H_{st} = aT + bT^2 + cT^{-1} + d$$

The values of a , b , c , and d were obtained using a least square method again by an IBM-7094 computer.

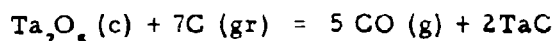
For some of the carbides whose heat capacity continues to increase rapidly even above room temperature, the empirical Kelley equation above does not adequately represent the data over the temperature range from 298.15°K to 3000°K with a single set of numerical coefficients. In such cases, the total temperature range was divided into two sub-ranges 298.15° to T , and T to 3000°K. The lower range was fitted to the four parameter Kelley equation above, and the upper range was fitted either with the same type of equation but with different parameters or to a reduced three parameter form:

$$H_T - H_{st} = a' T + b' T^2 + d'$$

Whenever the high-temperature heat content data have been evaluated by the JANAF group or Dr. Kelley of the Bureau of Mines, their tabulated data have been adopted in this compilation.

4. Reaction Equilibrium Data

The thermodynamic properties of a carbide phase may be conveniently obtained from solid-solid equilibria (the phase equilibria of more than two components) and solid-gas equilibria. For instance, for the reaction



the thermodynamic properties of TaC may be derived by measuring the vapor pressure of CO as a function of temperature above $\text{Ta}_2\text{O}_5\text{-C-TaC}$, when the related data of Ta_2O_5 , C and CO are known.

Whenever the free energy functions of all the reactants and products are known, the standard heat of reaction at 298.15°K may be calculated from each individual measurement using the following relationship:

$$\Delta H_{R, st} = - T (\Delta f_{ef}) + \Delta G_R$$

In the above equation, Δf_{ef} is the sum of the free energy functions of the products minus the sum of the free energy functions of the reactants. From an arithmetic average value of $\Delta H_{R, st}$ and knowing the heats of formation of all the other reactants and products, the heat of formation of this carbide phase was obtained. This value of $\Delta H_{f, st}$ was then compared with the value

derived from the vapor pressure measurements and with the direct calorimetric value, and then the value of $\Delta H_{f, st}$ was selected.

Whenever the values of $\Delta H_{R, st}$ derived from the equilibrium data show a trend with temperature, indications are that the reaction equilibrium as written may not be the true equilibrium. In such cases, the value of $\Delta H_{R, st}$ derived was not considered in the final selection of data.

5. Vapor Pressure Data

The vaporization behavior of a number of carbide phases has been studied using either the Knudsen technique or the Langmuir method. In either case, the data were evaluated using the Third Law method. For example, the vaporization of a monocarbide phase to gaseous elements may proceed as written below:



The thermodynamic properties of the MeC phase can then be obtained by measuring the partial pressures of Me and C above the MeC phase, provided the thermodynamic properties of Me and C are known. For each measurement, the heat of vaporization, $\Delta H_{v, st}$, for the MeC phase was calculated by the Third Law method. From an arithmetic average value of the $\Delta H_{v, st}$, the heat of formation of the MeC phase was obtained knowing the heats of vaporization of the elements.

Whenever an alloy phase does not vaporize congruently, the composition of this alloy phase within the homogeneous range during the course of evaporation is changing with time and so will the partial pressure of the more volatile component. Under such conditions, one cannot obtain meaningful data, unless the amount of the material vaporized is so small that the composition of the alloy phase does not change appreciably.

6. Calorimetric Data

The heats of formation of carbide phases have been generally determined by combustion calorimetry. Provided the sample used and the combustion products are defined, combustion calorimetry always yields more precise heat of formation values in comparison with other thermochemical methods.

7. Selection of Enthalpy and Free Energy Data

The value of the enthalpy (heat) of formation at 298.15°K, $\Delta H_{f, st}$, of a carbide phase together with an estimated uncertainty has been selected based on the values derived from the reaction equilibrium data, the vapor pressure data, and the calorimetric data. Using this selected value of $\Delta H_{f, st}$ and the available free energy functions for the carbide phase and the elements, the Gibbs free energy of formation, ΔG_f , of this carbide phase with a definite composition was calculated as a function of temperature.

The ΔG_f values as a function of temperature are presented as a linear function of temperature. Only for those cases, where ΔC_p values change drastically with temperature, an additional $T \log T$ term is added to the linear equation in order to represent the ΔG_f values adequately.

In the present compilation, the stable form of the element at any temperature and one atmosphere pressure has been adopted as its standard state.

B. EXPERIMENTAL THERMODYNAMIC PROPERTIES OF BINARY CARBIDES

1. Group IV-Metal Carbon Systems

In the systems of carbon with the three group IV transition metals titanium, zirconium and hafnium, only one intermediate phase, a monocarbide with B1-type of structure, is formed. The homogeneous range of this phase in all three systems is large and varies from about $x_C = 0.32$ to 0.5. At $x_C = 0.5$ both the metal lattice and the carbon sublattice are filled, but for $x_C < 0.5$, the carbon sublattice is deficient with carbon atoms. Most of the thermodynamic data reported in the literature for this compound refer to compositions at or close to stoichiometry. Many measurements were made on samples of undefined purity and stoichiometry.

In the following sections, the literature values were evaluated according to the methods described in section II-A and the most consistent values are selected. Also included in this compilation is an evaluation of the thermodynamic properties of hafnium, which was needed for the calculation of the thermodynamic quantities of the HfC phase.

a. Titanium-Carbon System

(1) Phase Diagram

The phase diagram as shown in Figure 1 was recently established by Rudy⁽²⁾ and co-workers. The only intermediate phase which is present, titanium monocarbide, exists over a wide range of homogeneity and melts congruently at 3067°C with a composition of ~44 atomic % carbon.

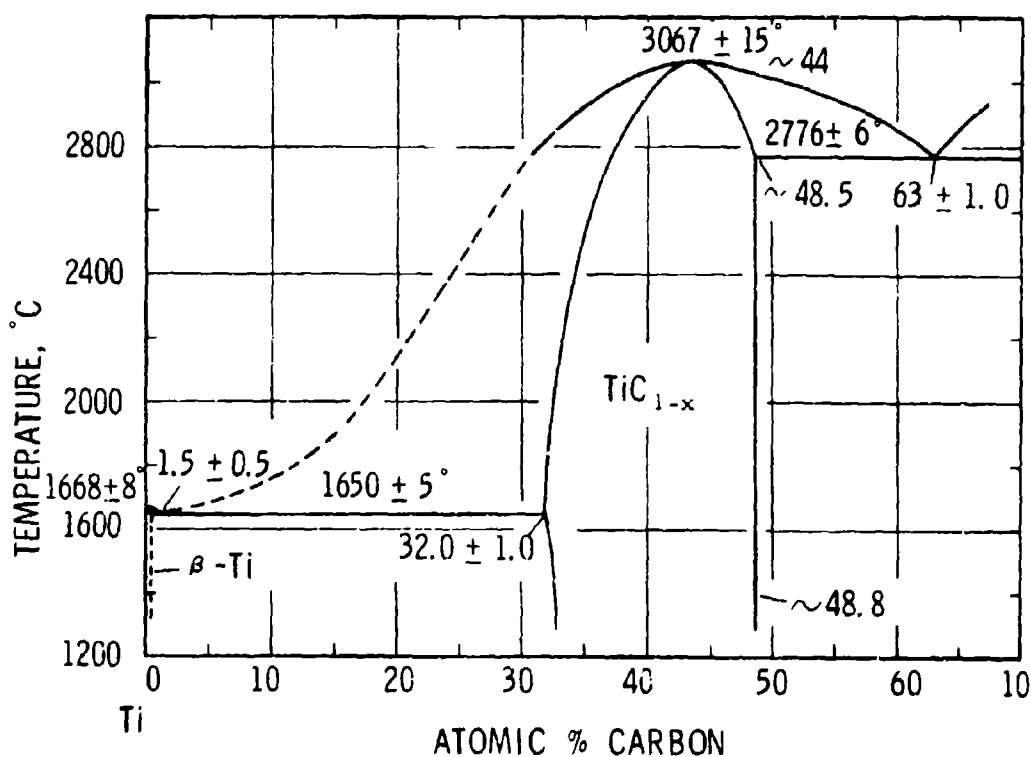


Figure 1. The Phase Diagram of the Titanium-Carbon System

(2) Low-Temperature Data

Kelley⁽³⁾ measured the low-temperature heat capacity of $\text{TiC}_{\sim 1.0}$ over the temperature interval 55° - 295°K. Integration of the heat capacity yielded the value of $S_{\text{at}} = 5.79 \pm 0.1$ cal/deg g-atom Ti. The sample used by Kelley had 3.12% metal impurities and 0.75% oxygen. Using the available entropies of titanium and graphite⁽⁴⁾, $\Delta S_{f, \text{st}} = -2.87 \pm 0.1$ cal/deg g-atom Ti was obtained.

(3) High-Temperature Data

Naylor⁽⁵⁾ measured the heat content of $\text{TiC}_{\sim 1.0}$ over the temperature interval 361 - 1735°K, and the sample used was prepared by reacting titanium with Norblack (99.7% carbon) in

vacuo at 1300 - 1350°C. Analysis of the sample showed 79.65% titanium and 19.85% carbon. The principal impurity was about 0.4% free titanium. Since TiC and TiO form a series of continuous solid solutions, one suspects the sample might also contain oxygen as impurity.

Neel⁽⁶⁾ measured the heat content of $\text{TiC}_{\sim 1.0}$ by means of an ice calorimeter over the temperature interval 590 - 2890°K. The chemical composition of the sample was 79.8% titanium, 19.2% carbon, and 0.9% nitrogen. Analysis of the heat content data of Neel showed a scatter of 22% at 1000°K (corresponding to about 750 cal/g-atom). Neel's smoothed value at 1800°K was about 14% higher than the value reported by Naylor.

Bender, et.al.⁽⁷⁾ determined C_p values of $\text{TiC}_{\sim 1.0}$ using a pulse-heating technique over the temperature interval 2000 - 2500°K. However, their average C_p value was about 14 cal/deg g-atom in comparison to 6.5 cal/deg g-atom obtained from Naylor's data. The data reported by Bender, et.al. are suspected to be in error.

From the foregoing discussion, it is concluded that the high-temperature thermal data of $\text{TiC}_{\sim 1.0}$ are not well-defined.

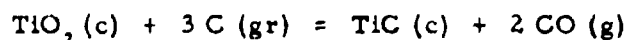
Based on the heat content data of Naylor, the high-temperature thermal properties of $\text{TiC}_{\sim 1.0}$ have been calculated and tabulated as part of the JANAF Thermochemical Tables. The heat content of $\text{TiC}_{\sim 1.0}$ over the temperature interval 298.15 - 2000°K as tabulated in the JANAF Tables may be represented by the following analytical

equation with an average standard deviation of 15 cal/g-atom Ti and a maximum deviation of 31 cal/g-atom Ti at 400°K.

$$H_T - H_{st} = 12.387 T + 1.6737 \times 10^{-4} T^2 + 4.2442 \times 10^{-5} T^3 - 5128.7$$

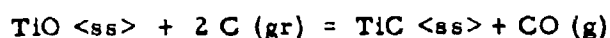
(4) Reaction Equilibrium Data

Brantley and Beckman⁽⁸⁾ studied the equilibrium TiO_2 -C-TiC-CO over the temperature interval 1278 - 1428°K. From X-ray analysis, they concluded that the solid phases consisted of TiO_2 , TiC only and no TiO. Thermodynamic calculations at 1323°K using the Gibbs free energies of formation of TiO_2 , TiO, and CO selected by Elliott and Gleiser⁽⁹⁾ showed that $x_{TiO} = 0.0005$ in the Ti(C,O) solid solution. This confirmed the conclusions of Brantley and Beckman. Using the values of the free energy function for CO, TiC, C and TiO_2 given in JANAF Thermochemical Tables⁽⁴⁾, the standard heat of reaction at 298.15°K, $\Delta H_{R, st}$ for the following reaction



was calculated to be $110,600 \pm 2440$ cal. The uncertainty includes only the scattering of the experimental measurements, not the uncertainties associated with the free energy functions. Again using the heats of formation of CO and TiO_2 given in JANAF Thermochemical Tables, $\Delta H_{f, st} = -62,070$ cal/g-atom Ti was obtained. This value of -62,070 cal/g-atom Ti is much more exothermic than the calorimetric result. Moreover, the heat of reaction calculated using the Third Law method showed a trend with temperature, i.e. with increasing temperature, the heat of reaction becomes more endothermic.

Kutsev and Ormont⁽¹⁰⁾ studied the equilibrium C-Ti(C,O)-CO over the temperature interval 1880-2600°K, with the partial pressure of CO varying from 20 mm to 750 mm Hg. The composition of TiO varied from 0.01 to about 0.1 mole fraction. Knowing the partial pressure of CO and the composition of TiO in Ti(C,O) solid solutions, and assuming ideal solution behavior, one can calculate the equilibrium constant of the following reaction:



A calculation at 2000°K yielded $\Delta G_R = 5,360 \pm 2600$ cal. Using the free energies of formation of TiO and CO from Elliott and Gleiser⁽⁹⁾, one obtained $\Delta G_{f, 2000^\circ\text{K}} = -17,000$ cal/g-atom Ti for $\text{TiC}_{\sim 1.0}$. This is only about half of the value selected as discussed in the latter section. We believe the error is due to the difficulty in the compositional analysis of the Ti(C,O) solid solution.

(5) Vapor Pressure Data

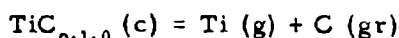
From a mass spectrometric study of TiC at about 2500°K, Chupka, Berkowitz, Glese and Inghram⁽¹¹⁾ found that there was no TiC molecule in the vapor phase.

Fujishiro and Gokcen⁽¹²⁾ measured the vapor pressure of titanium over TiC-C over the temperature interval 2383 - 2593°K using the Knudsen technique. A Third Law evaluation of their vapor pressure data yielded $\Delta H_{f, \text{st}} = -31,330$ cal/g-atom Ti. This value is about 12,000 cal less exothermic than the calorimetric value. We believe that the data of Fujishiro and Gokcen are in error because of

the fact that the weight loss of the empty Knudsen cell was about two to three times larger than the actual weight loss of the sample.

Coffman, Kibler, Lyon, and Acchione⁽¹³⁾ studied the Langmuir vaporization of $\text{TiC}_{\sim 1.0}$ over the temperature interval 2100 - 2542°K. They concluded that $\text{TiC}_{\sim 1.0}$ vaporized congruently in their experiment based on the fact that the lattice parameter of $\text{TiC}_{\sim 1.0}$ remained constant with the amount of material vaporized. Using the available values of the free energy function for $\text{TiC}_{\sim 1.0}$, C, and $\text{Ti}^{(4)}$, Coffman, et.al. obtained $\Delta H_{v, st} = 326,200 \pm 1,200$ cal/g-atom Ti, which yielded $\Delta H_{f, st} = -42,800 \pm 1400$ cal/g-atom Ti for $\text{TiC}_{\sim 1.0}$, in reasonable agreement with the calorimetric value.

Using the resonance line absorption technique, Coffman, et.al.⁽¹³⁾ found the vapor pressure of Ti over TiC and graphite at 2200°K to be the same as that of pure Ti at 1660°K. From this information, they obtained $\Delta G_{R, 2200^\circ K} = 74,130$ cal for the following reaction:



Using the available free energy functions for $\text{TiC}_{\sim 1.0}$, Ti and C, and the heat of vaporization of Ti, they derived $\Delta H_{f, st} = -42,700$ cal/g-atom Ti, again in reasonable agreement with the direct calorimetric data.

Bolgar, Verkhoglyadova and Samsonov⁽¹⁴⁾ concluded that there was a molecular species, TiC , which decomposed just after leaving the surface from the Langmuir experiment. However, their results are doubtful as pointed out by Storms⁽¹⁵⁾.

(6) Calorimetric Data

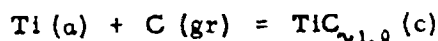
Humphrey⁽¹⁶⁾ measured the heat of combustion of TiC using combustion calorimetry and obtained $\Delta H_{f, st} = -43,900 \pm 400$ cal/g-atom Ti. The sample was the same one used by Naylor for heat content measurements. Lowell and Williams⁽¹⁷⁾ determined the heat of formation of $TiC_{\sim 1.0}$ by direct reaction of the elements at high temperature and obtained a value of $-43,800 \pm 4000$ cal/g-atom Ti. The uncertainty of the measurements is rather large.

(7) Selection of Enthalpy and Free Energy Data

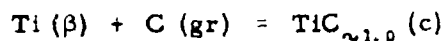
The heat of formation of $TiC_{\sim 1.0}$ at 298.15°K was selected to be $-43,100 \pm 2000$ cal/g-atom Ti based on the following three values:

| <u>Investigator</u> | <u>Method</u> | <u>$\Delta H_{f, st}$</u> |
|---------------------|--------------------------------------|--------------------------------------|
| Humphrey | Combustion Calorimetry | $-43,900 \pm 400$ |
| Coffman, et.al. | Resonance line Absorption, 2200°K | $-42,700$ |
| Coffman, et.al. | Langmuir, 2210 - 2542°K | $-42,800 \pm 1400$ |
| Selected Value | | $-43,100 \pm 2000$ |

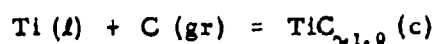
With the selected value of $\Delta H_{f, st}$ for $TiC_{\sim 1.0}$ and the available free energy functions of $TiC_{\sim 1.0}$, Ti, and C, the Gibbs free energy of formation of $TiC_{\sim 1.0}$ as a function of temperature can be calculated. The calculated ΔG_f values as a function of temperature were fitted to three linear equations and these equations are:



$$\Delta G_{f, 298.15 - 1155^\circ \text{K}} = -42,890 + 2.44 T$$



$$\Delta G_{f, 1155 - 1940^\circ \text{K}} = -44,220 + 3.57 T$$



$$\Delta G_{f, 1940 - 3000^\circ \text{K}} = -48,490 + 5.77 T$$

b. Zirconium-Carbon System

(1) Phase Diagram

The phase diagram as shown in Figure 2 was established by Sara, Lowell, and Dolloff⁽¹⁸⁾ and more recently by Rudy⁽²⁾ and co-workers. Similar to the behavior of titanium monocarbide, zirconium monocarbide also exists over a wide range of homogeneity and melts congruently at 3440°C with a composition of 45 atomic % carbon.

(2) Low-Temperature Data

Westrum and Felck⁽¹⁹⁾ measured the low-temperature heat capacity of $\text{ZrC}_{\sim 1.0}$ over the temperature interval 5.59 - 345.16°K. Integration of the heat capacity yielded the value of $S_{\text{st}} = 7.90 \pm 0.02$ cal/deg g-atom Zr for $\text{ZrC}_{\sim 1.0}$. According to the authors, the approximate compositions of the sample by weight was 96.5% ZrC, 2.4% Zr, 0.5% ZrN, 0.4% ZrB₂ and 0.15% TiC. Using the available

entropies of zirconium⁽⁴⁾ and graphite⁽⁴⁾,

$$\Delta S_{f, st} = -2.75 \pm 0.05 \text{ cal/deg g-atom Zr}$$

was obtained.

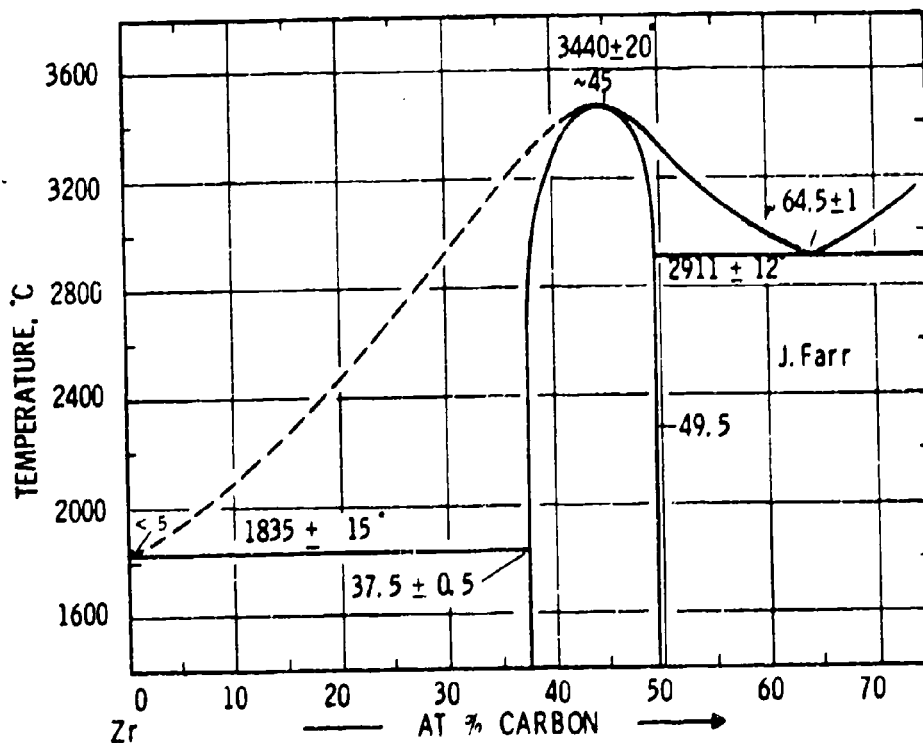


Figure 3. Phase Diagram of the Zirconium-Carbon System

(3) High-Temperature Data

Mezaki, Jambois, Gangopadhyay,

and Margrave⁽²⁰⁾ measured the heat content of $ZrC_{\sim 1.0}$ over the temperature interval 480 - 1170°K using the same material as Westrum and Feick did for their low-temperature heat-capacity measurement. Analysis of the data of Mezaki, et.al. showed a scattering of $\pm 1\%$ with the exception at one temperature, $\pm 5\%$.

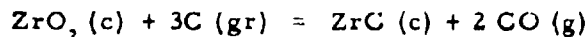
Bender, et.al.⁽⁷⁾ determined the C_p of 94.7% ZrC over the temperature interval 1640 - 2370°K and obtained an average C_p of about 10 cal/deg g-atom alloy which we believe is too high.

Based on the data of Mezaki, et.al. from 480 to 1170°K, of Neel⁽⁶⁾ from 600 to 3000°K, and of McDonald, Oetting and Prophet⁽²¹⁾, the high-temperature thermal properties of $ZrC_{1.0}$ have been calculated as part of the JANAF Thermochemical Tables. The heat content of $ZrC_{1.0}$ as tabulated in the JANAF Tables over the temperature interval 298.15 - 3000°K may be represented by the following analytical expression with an average deviation of 6 cal/g-atom Zr and a maximum deviation of 16 cal/g-atom Zr at 3000°K:

$$H_T - H_{st} = 12.411 T + 3.5303 \times 10^{-4} T^2 + 3.5317 \times 10^{-8} T^{-1} - 4915.9$$

(4) Reaction Equilibrium Data

Prescott⁽²²⁾ studied the equilibrium ZrO_2 -C-ZrC-CO over the temperature interval 1800 - 2015°K. From X-ray analysis, Prescott concluded that the solid phases consisted of ZrO_2 , C, and ZrC. Using the free energy functions for CO, ZrC, C, and ZrO_2 given in the JANAF Thermochemical Tables⁽⁴⁾, the standard heat of reaction at 298.15°K, $\Delta H_{R,st}$, for the following reaction:

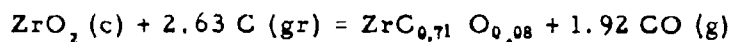


is calculated to be $162,616 \pm 390$ cal. The uncertainty in $\Delta H_{R,st}$ includes only the scatter in the experimental values of the vapor pressure of CO

above $\text{ZrO}_2\text{-C-ZrC}$ but does not include the uncertainties in the values of the free energy function. Again using the available heats of formation of $\text{CO}^{(4)}$ and $\text{ZrO}_2^{(4)}$, $\Delta H_{f, \text{st}}$ of $\text{ZrC}_{\sim 1.0}$ was calculated to be -46,050 cal/g-atom Zr, which is in reasonable agreement with the calorimetric value and the values derived from vapor pressure data.

Kutsev, Ormont, and Epelbaum⁽²³⁾

studied the same equilibrium over the temperature interval 1814 - 2020°K, but found the vapor pressure of CO only about half the value reported by Prescott. From X-ray and chemical analysis, Kutsev, et.al. concluded that they were studying the reaction:



Recently, Hollahan and Gregory

measured the equilibrium vapor pressure of CO above $\text{ZrO}_2\text{-C-ZrC}$ over the temperature interval 1422 - 1520°K using the torsion effusion technique. Using the Second Law treatment of their data, Hollahan and Gregory⁽²⁴⁾ obtained a value of 147,000 cal as the apparent heat of reaction between ZrO_2 and graphite to form ZrC and CO. The value of 147,000 cal is much different from the value obtained from Prescott's data. Since the individual experimental data were not tabulated in the original paper of Hollahan and Gregory, a Third-Law treatment of their data was not made.

In view of the discrepancy between the three different equilibrium measurements, the heat of formation of $\text{ZrC}_{\sim 1.0}$ derived from the equilibrium data was not considered in the final selection of thermodynamic data of $\text{ZrC}_{\sim 1.0}$.

(5) Vapor Pressure Data

Pollock⁽²⁵⁾ measured the vapor pressure of zirconium over ZrC and graphite using a Knudsen cell over the temperature interval 2620 - 2730°K. Using the values of the free energy function given in JANAF Thermochemical Tables⁽⁴⁾, the heat of vaporization of $\text{ZrC}_{\sim 1.0}$ at 298.15°K was calculated to be $192,300 \pm 1000$ cal/g-atom Zr. Knowing the heat of vaporization of zirconium,

$$\Delta H_{f, st} = -46,500 \pm 200 \text{ cal/g-atom Zr}$$

was obtained for $\text{ZrC}_{\sim 1.0}$.

Pollock⁽²⁵⁾ also studied the vaporization of $\text{ZrC}_{\sim 1.0}$ to gaseous zirconium and carbon over the temperature interval 2640 - 2745°K using the Langmuir method. The heat of vaporization of $\text{ZrC}_{\sim 1.0}$ in this case was calculated to be $363,770 \pm 700$ cal/g-atom Zr. This result yielded $\Delta H_{f, st} = -47,060 \pm 1870$ cal/g-atom Zr for $\text{ZrC}_{\sim 1.0}$.

Coffman, Kibler, Lyon, and

Acciione⁽¹³⁾ studied the vaporization of $\text{ZrC}_{\sim 1.0}$ over the temperature interval 2351 - 2898°K using the Langmuir method. The standard heat of vaporization of $\text{ZrC}_{\sim 1.0}$ was calculated to be $363,497 \pm 1550$ cal/g-atom Zr, in good agreement with Pollock's Langmuir result. Again using the available heats of vaporization of zirconium and carbon,

$$\Delta H_{f, st} = -46,810 \pm 2300 \text{ cal/g-atom Zr}$$

was obtained. Coffman, et.al. concluded that $\text{ZrC}_{\sim 1.0}$ vaporized congruently based on the fact that the lattice parameter of $\text{ZrC}_{\sim 1.0}$ remained constant with the amount of material vaporized.

Using the resonance-line absorption technique, Coffman, et.al.⁽¹³⁾ found the vapor pressure of Zr over $\text{ZrC}_{\sim 1.0}$ and graphite at 2740°K to be the same as that of pure Zr at 2144°K. Knowing the vapor pressure of Zr over ZrC and graphite at 2740°K, the standard heat of vaporization of ZrC at 298.15°K was calculated to be 192,430 cal/g-atom Zr, again in good agreement with Pollock's Knudsen experimental result. From this value, $\Delta H_{f, st} = -46,630$ cal/g-atom Zr was obtained for $\text{ZrC}_{\sim 1.0}$.

The uncertainties associated with the calculated heats of vaporization of $\text{ZrC}_{\sim 1.0}$ discussed in the previous sections include only the scattering of the individual vapor pressure data, while the uncertainties associated with the derived heat of formation value for $\text{ZrC}_{\sim 1.0}$ include the uncertainties in the vapor pressure data, the free energy functions and the heats of vaporization of the elements involved.

(6) Calorimetric Data

Mah and Boyle⁽²⁶⁾ measured the heat of combustion of $\text{ZrC}_{\sim 1.0}$ calorimetrically and obtained

$$\Delta H_{f, st} = -44,100 \pm 1500 \text{ cal/g-atom Zr.}$$

The $\text{ZrC}_{\sim 1.0}$ sample was prepared by directly reacting zirconium with graphite and had an unaccounted impurity of 0.78% which was assumed to be nitrogen and oxygen.

More recently Mah⁽²⁷⁾ redetermined the heat of combustion of relatively pure $\text{ZrC}_{\sim 1.0}$ sample supplied by Union Carbide Research Institute and A. D. Little, Inc. The combustion

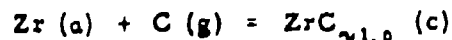
results from the two different samples agreed with each other and yielded $\Delta H_{f, st} = -47,000 \pm 600$ cal/g-atom Zr. In the same report, Mah also determined the heat of formation of $ZrC_{0.70}$ to be $-33,100 \pm 800$ cal/g-atom Zr. The discrepancy between the two different calorimetric measurements is probably due to the unaccounted impurities in the sample used by Mah and Boyle.

(7) Selection of Enthalpy and Free Energy Data

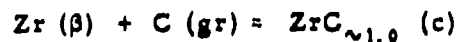
The heat of formation of $ZrC_{1.0}$ at 298.15°K was selected to be $-46,800 \pm 1000$ cal/g-atom Zr based on the following five values. The calorimetric value of Mah was given a weight of four while all the other four values were given a weight of only one.

| <u>Investigator</u> | <u>Method</u> | <u>$\Delta H_{f, st}$</u> |
|---------------------|-------------------------------------|--------------------------------------|
| Mah | Combustion Calorimetry | $-47,000 \pm 600$ |
| Pollock | Knudsen, 2620 - 273°K | $-46,500 \pm 2000$ |
| Pollock | Langmuir, 2647 - 2673°K | $-47,060 \pm 1900$ |
| Coffman, et.al. | Resonance-line Absorption 2740°K | $-46,630$ |
| Coffman, et.al. | Langmuir, 2246 - 2898°K | $-46,810 \pm 2300$ |
| Selected Value | | $-46,800 \pm 1000$ |

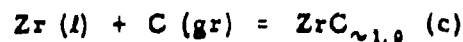
Using the selected value of $\Delta H_{f, st}$ for $ZrC_{1.0}$, and the available free energy functions of $ZrC_{1.0}$, Zr and graphite, the Gibbs free energy of formation of $ZrC_{1.0}$ was calculated. The calculated ΔG_f values as a function of temperature were fitted to three linear equations and these equations are:



$$\Delta G_{f, 298.15 - 1147^\circ\text{K}} = -46,500 + 1.61 T$$



$$\Delta G_{f, 1149 - 2225^\circ\text{K}} = -47,760 + 2.71 T$$



$$\Delta G_{f, 2125 - 3000^\circ\text{K}} = -51,220 + 4.34 T$$

c. Hafnium

(1) Low-Temperature Data

Westrum⁽²⁸⁾ measured the low-temperature heat capacity of hafnium over the temperature interval 5.82 - 348.55°K and reported tentative values of $S_{st} = 6.140$ cal/deg g-atom and $H_{st} - H_0 = 1224.0$ cal/g-atom.

(2) High-Temperature Data

Hawkins, Onillon and Orr⁽²⁹⁾ measured the high-temperature heat content of hafnium over the temperature interval 298 - 1346°K. The sample used by Hawkins, et.al. contained 2.8% Zr, and less than a total of 0.055% of remaining impurities, principally 0.02% Fe, 0.010% Ni and 0.008% O. The heat content values of hafnium were derived by the authors from the measured values for the zirconium impurity assuming that Kopp's law of additivity applied.

Since there are no experimental heat content values of hafnium above 1346°K, we assume that Y as defined earlier increases linearly with temperatures above 1346°K up to the α (hcp) \rightarrow β (bcc) transformation temperature based on the fact that Y varies linearly with temperature below 1346°K.

The α - β transformation temperature is not well-established at the present. Recently Rudy and co-workers⁽²⁾ of our laboratory determined the α - β transformation temperature and the melting temperature of hafnium containing four atomic percent zirconium to be 2073°K and 2491°K respectively. In this evaluation we have adopted these values as the transformation and melting temperatures of pure hafnium until better data become available. Since no thermal data are available for the bcc and liquid phases of hafnium, we have assumed that $\Delta S^{\alpha \rightarrow \beta}$ and $\Delta S^{\beta \rightarrow L}$ are 0.90 and 2.3 cal/deg g-atom respectively, and that the values of C_p for the bcc phase and liquid phase are constant and equal to 8.6 and 8.0 cal/deg g-atom respectively.

The calculated high-temperature thermal properties of hafnium are reported in Table 1 and the estimated values are parenthesized. The heat content of α -Hf over the temperature interval 298.15 - 2073°K as tabulated may be represented by the following analytical expression with an average standard deviation of 0.5 cal/deg g-atom and a maximum deviation of 1 cal/deg g-atom at 2073°K:

$$H_T - H_{298} = 5.5776 T + 0.92474 \times 10^{-3} T^2 - 0.030942 \times 10^{-6} T^3 - 1734.8$$

Table 1. High-Temperature Thermal Properties of Hafnium

| T°K | C _p | H _T -H _{st} | S _T -S _{st} | $-\frac{G_T-H_{st}}{T}$ | log P |
|---------|----------------|---------------------------------|---------------------------------|-------------------------|---------|
| 298.15 | 6.15 | 0 | 0.00 | 10.41 | -101.48 |
| 400 | 6.34 | 636 | 1.83 | 10.65 | - 73.35 |
| 500 | 6.52 | 1278 | 3.26 | 11.11 | - 57.52 |
| 600 | 6.70 | 1939 | 4.47 | 11.65 | - 46.72 |
| 700 | 6.88 | 2618 | 5.52 | 12.19 | - 39.01 |
| 800 | 7.06 | 3316 | 6.45 | 12.71 | - 33.23 |
| 900 | 7.25 | 4031 | 7.29 | 13.22 | - 28.74 |
| 1000 | 7.43 | 4765 | 8.06 | 13.71 | - 25.15 |
| 1100 | 7.61 | 5517 | 8.78 | 14.17 | - 22.22 |
| 1200 | 7.79 | 6287 | 9.45 | 14.62 | - 19.78 |
| 1300 | 7.98 | 7076 | 10.08 | 15.05 | - 17.71 |
| 1400 | (8.16) | (7884) | (10.67) | (15.45) | - 15.94 |
| 1500 | (8.35) | (8710) | (11.25) | (15.85) | - 14.41 |
| 1600 | (8.53) | (9555) | (11.92) | (16.36) | - 13.10 |
| 1800 | (8.90) | (11299) | (12.82) | (16.95) | - 10.84 |
| 2000 | (9.27) | (13117) | (13.77) | (17.62) | - 9.06 |
| 2073(α) | (9.38) | (13801) | (14.11) | | |
| 2073(β) | (8.6) | (15671) | (15.01) | (17.86) | - 8.50 |
| 2200 | (8.6) | (16763) | (15.52) | (18.31) | - 7.62 |
| 2400 | (8.6) | (18481) | (16.27) | (18.98) | - 6.43 |
| 2491(β) | (8.0) | (19216) | (16.59) | | |
| 2491(I) | (8.0) | (24945) | (18.89) | (19.27) | - 5.96 |
| 2600 | (8.0) | (25867) | (19.23) | (19.69) | - 5.44 |
| 2800 | (8.0) | (27467) | (19.83) | (20.43) | - 4.62 |
| 3000 | (8.0) | (29067) | (20.38) | (21.10) | - 3.90 |

(3) Vapor Pressure Data

Blackburn⁽³⁰⁾; Panish and Reif⁽³¹⁾; and Kibler, Lyon, Linevsky and DeSantis⁽³²⁾ measured the vapor pressure of hafnium using the Langmuir method. The sample used by Blackburn contained 468 ppm O, 270 ppm Zr and 150 ppm Nb; the sample used by Panish and Reif had 400 ppm O; and the sample used by Kibler, et.al. contained 69 ppm O, 81 ppm N, 3 ppm H, 1.93% Zr and traces of Fe, Mg and Ti.

Application of the Third Law test to the vapor pressure data yielded the following heats of vaporization of hafnium:

| <u>Investigator</u> | <u>$\Delta H_{v, at}$</u> |
|--------------------------------|--------------------------------------|
| Blackburn, 2200 - 2363°K | 149,200 \pm 650 |
| Panish and Reif, 2066 - 2274°K | 145,590 \pm 1400 |
| Kibler, et.al., 2035 - 2325°K | 148,100 \pm 300 |
| Selected Value | 148,650 \pm 2500 |

The selected value of $\Delta H_{v, at}$ is the average of the first and third values with an estimated uncertainty of 2500 cal/g-atom. The uncertainties associated with the individual values include only the scatter of the vapor pressure data, but do not include the uncertainties of the free energy functions.

Using this value of $\Delta H_{v, at}$, the values of the free energy function for the condensed phase in Table 1, and those for

the gas phase from Hultgren, et.al.⁽¹⁾, the values of the log P were calculated and are tabulated in Table 1.

d. Hafnium-Carbon System

(1) Phase Diagram

The phase diagram as shown in Figure 3 was established by Rudy⁽²⁾ and co-workers. In contrast to

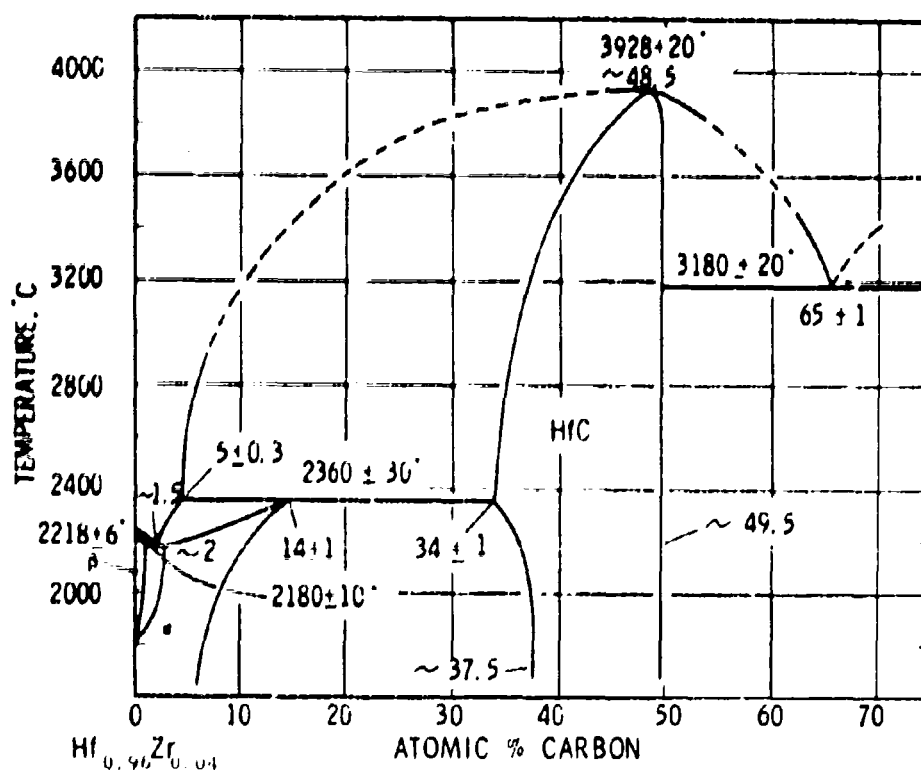


Figure 3. The Phase Diagram of the Hafnium-Carbon System

titanium-carbon and zirconium-carbon systems, the addition of carbon atoms to α -Hf stabilizes the α -terminal solid solution to high temperatures

where the pure α -Hf is unstable with respect to the β -Hf. The only intermediate phase, hafnium carbide, exists over a wide range of homogeneity and melts congruently at 3928°C with a composition of 48.5 atomic % carbon.

(2) Low-Temperature Data

Westrum⁽²⁸⁾ measured the low-temperature heat capacity of $\text{HfC}_{\sim 1.0}$ over the temperature interval 5.09 - 350.0°K. The sample was prepared by arc-melting in an atmosphere of argon containing 3.14% ethylene and 11.4% hydrogen. From the heat capacity data, Westrum reported a tentative value of

$$S_{st} = 9.431 \text{ cal/deg. g-atom Hf.}$$

Using the entropy of Hf selected in the previous section and the entropy of graphite from JANAF Thermochemical Tables,

$$\Delta S_{f, st} = -2.34 \pm 0.05 \text{ cal/deg g-atom Hf}$$

was obtained.

(3) High-Temperature Data

The high-temperature values selected for $\text{HfC}_{\sim 1.0}$ are based on the heat content of Coffman, et.al.⁽¹³⁾ over the temperature interval 440 - 1378°K, and of Levinson⁽³³⁾ over the temperature interval 1286 - 2805°K. The selected values join smoothly with the low-temperature heat capacity. The data of Coffman, et.al. scatter by about $\pm 3\%$ above 800°K, but scatter much more below this temperature, while the data of Levinson scatter by about only $\pm 1\%$.

The sample used by Coffman, et.al. had the following impurities: 0.39% free C, 0.05% N, 0.011% H, 4.0% Zr, 0.01% Fe, and 0.005% Ti and the heat content values were corrected for the zirconium impurity. On the other hand, the sample used by Levinson was much purer, containing only 100 ppm Fe, less than 500 ppm free C, and less than 400 ppm Zr, and consequently no correction in the measured heat content values was necessary.

Neel⁽⁶⁾ also measured the heat content of HfC (purity unknown) over the temperature interval 540 - 3016°K, but his data scattered wildly over the whole temperature range and were not considered in the selection.

Based on the selected values of Y, the calculated high-temperature thermal properties of HfC_{1.0} are reported in Table 2, and the heat content over the temperature interval 298.15 - 1000°K may be represented by the following analytical expression with an average standard deviation of 10 cal/g-atom Hf and a maximum deviation of 17 cal/g-atom Hf at 1000°K:

$$H_T - H_{st} = 10.346 T + 11.245 \times 10^{-4} T^2 + 2.0796 \times 10^{-5} T^{-1} - 3881.0$$

From 1000°K to 3000°K, the heat contents of HfC_{1.0} may be represented by the second analytical expression below with an average standard deviation of 6 cal/g-atom Hf and a maximum deviation of 10 cal/g-atom Hf at 2100°K:

$$H_T - H_{st} = 11.196T + 5.9671 \times 10^{-4} T^2 - 3970.0$$

Table 2. High-Temperature Thermal Properties of $\text{HfC}_{\sim 1.0}$

| T°K | C_p | $H_T - H_{st}$ | $S_T - S_{st}$ | $-\frac{G_T - H_{st}}{T}$ |
|--------|-------|----------------|----------------|---------------------------|
| 298.15 | 8.96 | 0 | 0.00 | 9.43 |
| 400 | 10.00 | 972 | 2.80 | 11.80 |
| 500 | 10.58 | 1996 | 5.08 | 10.52 |
| 600 | 11.03 | 3071 | 7.04 | 11.35 |
| 700 | 11.43 | 4195 | 8.77 | 12.21 |
| 800 | 11.78 | 5365 | 10.33 | 13.06 |
| 900 | 12.07 | 6573 | 11.76 | 13.88 |
| 1000 | 12.28 | 7814 | 13.06 | 14.68 |
| 1100 | 12.46 | 9068 | 14.26 | 15.44 |
| 1200 | 12.61 | 10333 | 15.36 | 16.18 |
| 1300 | 12.75 | 11601 | 17.37 | 16.88 |
| 1400 | 12.87 | 12881 | 17.32 | 17.55 |
| 1500 | 12.99 | 14170 | 18.21 | 18.19 |
| 1600 | 13.10 | 15478 | 19.05 | 18.81 |
| 1700 | 13.23 | 16791 | 19.85 | 19.40 |
| 1800 | 13.35 | 18114 | 20.61 | 19.97 |
| 1900 | 13.46 | 19451 | 21.33 | 20.52 |
| 2000 | 13.58 | 20803 | 22.02 | 21.05 |
| 2100 | 13.70 | 22163 | 22.69 | 21.56 |
| 2200 | 13.82 | 23545 | 23.33 | 22.06 |
| 2300 | 13.94 | 24933 | 23.95 | 22.54 |
| 2400 | 14.05 | 26338 | 24.54 | 23.00 |
| 2500 | 14.17 | 27748 | 25.12 | 23.45 |
| 2600 | 14.29 | 29178 | 25.68 | 23.89 |
| 2700 | 14.40 | 30612 | 26.22 | 24.32 |
| 2800 | 14.53 | 32059 | 26.75 | 24.73 |
| 2900 | 14.64 | 33512 | 27.26 | 25.13 |
| 3000 | 14.77 | 34992 | 27.76 | 25.53 |

(4) Reaction Equilibrium Data

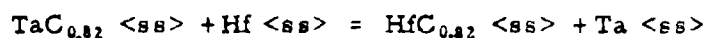
Zhelankin, Kutsev and Ormont^(34,35)

studied the equilibrium $\text{HfO}_2\text{-C-HfC}_{0.95}\text{O}_{0.05}\text{-CO}$ over the temperature interval 1743 - 2003°K. Since there is reliable calorimetric value for $\text{HfC}_{1.0}$, we have not evaluated the equilibrium data of Zhelankin, et.al. Moreover, this kind of measurement did not yield any reliable thermodynamic data for TiC and ZrC as discussed in the previous sections.

Rudy and Nowotny⁽³⁶⁾ evaluated the

Hf-Ta-C phase diagram thermodynamically at 2123°K and obtained

$\Delta G_{R, 2123^\circ\text{K}} = -8500 \text{ cal/g-atom Hf}$ for the following reaction:



(5) Vapor Pressure Data

Blackburn⁽³⁰⁾ studied the vaporization

behavior of $\text{HfC}_{0.97}$ by Langmuir method and reported tentative vapor pressure data at two temperatures, 2800 and 2890°K. The Third Law test of his data yielded $\Delta H_{v, \text{st}} = 369,790 \text{ cal} \pm 1630 \text{ cal/g-atom Hf}$. As pointed out by Blackburn, because of possible temperature errors, there is an uncertainty of $\pm 7 \text{ kcal}$ in the heat of vaporization value.

Coffman, Kibler, Lyon and Acchione⁽¹³⁾

measured the vapor pressures of Hf and C above HfC over the temperature interval 2313 - 3145°K. The sample was the same one they used to measure the heat content of HfC as discussed in the previous section. The Third Law treatment of their data yielded $\Delta H_{v, \text{st}} = 379,470 \pm 2500 \text{ cal/g-atom Hf}$. Again the uncertainty included only the scattering of the vapor pressure

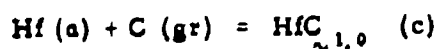
data and did not include the uncertainties in the values of the free energy function. Using the value of $\Delta H_{f, st}$ for Hf selected in this compilation and that for graphite from JANAF Thermochemical Tables, we obtained $\Delta H_{f, st} = -59,900$ cal/g-atom Hf for HfC. This value is much more exothermic than the direct calorimetric value. We believe the value derived from the vapor pressure data to be in error since there are uncertainties not only in the vapor pressure data of HfC and Hf, but also in the high-temperature thermal properties of pure hafnium.

(6) Calorimetric Data

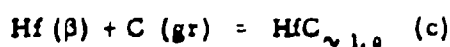
Mah ⁽²⁷⁾ determined the heat of formation of HfC_{1.0} by combustion calorimetry. The sample used by Mah was supplied by L. A. McClaine and had the following chemical analysis: 93.84% Hf, 6.02% combined C, 0.06% free C, 0.035% Zr, 0.031 N, 0.005% Fe, 0.003% O, 0.002% each of Si and Ti and 0.001% each of Cu, H, Mg and Mn. The heat of formation of HfC_{1.0} obtained by Mah is $-52,300 \pm 400$ cal/g-atom Hf.

(7) Selection of Enthalpy and Free Energy Data

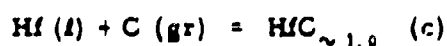
The heat of formation of HfC_{1.0} at 298.15°K was selected to be $-52,300 \pm 1500$ cal/g-atom Hf based solely on the calorimetric value. With this value of $\Delta H_{f, st}$ for HfC_{1.0} and the available free energy functions of HfC_{1.0}, Hf and graphite, the Gibbs free energy of formation of HfC_{1.0} was calculated. The calculated ΔG_f values as a function of temperature were fitted to three linear equations and these equations are:



$$\Delta G_{f, 29815 - 2073^\circ\text{K}} = -52,350 + 2.08 \text{ T}$$



$$\Delta G_{f, 2073 - 2491^\circ\text{K}} = -55,630 + 3.66 \text{ T}$$



$$\Delta G_{f, 2491 - 3000^\circ\text{K}} = -60,730 + 5.71 \text{ T}$$

2. Group V Metal Carbon Systems

In addition to forming the monocarbide (B1 type), the three group V metals, vanadium, niobium, and tantalum form a second intermediate phase with carbon having a stoichiometric composition corresponding to Me_3C phase. While the range of homogeneity in the monocarbide phases is comparable to that of the group IV carbides, the homogeneous range in the subcarbide Me_3C is relatively narrow in the lower temperature range.

For niobium-carbon and tantalum-carbon systems, there is a high-temperature polymorphic form of the Me_3C phase whose range of homogeneity is rather large⁽²⁾. Between the Me_3C and MeC phases, there also exists a metastable ζ phase.

a. Vanadium-Carbon System

(1) Phase Diagram

The phase diagram as shown in Figure 4 was established by Storme and McNeal⁽³⁷⁾.

6.59 ± 0.1 cal/deg g-atom V. Using the value of $S_{st} = 6.88 \pm 0.05$ cal/deg g-atom for V as reported by Bieganski and Stalinski⁽³⁹⁾ and that of graphite from JANAF Thermochemical Tables, $\Delta S_{f, st} = -1.47 \pm 0.12$ cal/deg g-atom V. was obtained.

(3) High-Temperature Data

King⁽⁴⁰⁾ measured the high-temperature heat contents of $VC_{0.87}$ over the temperature interval 397.2 - 1611°K. The sample used was the same one used by Shomate and Kelley for the determination of the low-temperature heat capacities. Assuming that the sample consisted of $VC_{0.87}$ and free carbon, the high-temperature thermal properties were calculated and are summarized in Table 3. The heat contents of $VC_{0.87}$ over the temperature interval 298.15 - 2000°K as reported in Table 3 may be represented by the following analytical expression with an average standard deviation of 32 cal/g-atom V and a maximum deviation of 75 cal/g-atom V at 400°K:

$$H_T - H_{st} = 10.547 T + 0.81848 \times 10^{-3} T^2 + 4.1753 \times 10^{-5} T^3 - 4612.8$$

(4) Reaction Equilibrium Data

Worrell and Chipman⁽⁴¹⁾ studied the equilibrium $V_2O_3 - V(C, O)_x - C - CO$ over the temperature interval 1200 - 1350°K, with a value of x varying between 0.88 and 1.2. The values of x in the equilibrium phase, which affects the derived enthalpy and free energy data for the monocarbide phase, could not be ascertained in the experiments.

Table 3. High-Temperature Thermal Properties of VC_{0.87}

| T°K | C _p | H _T -H _{st} | S _T -S _{st} | $-\frac{G_T-H_{st}}{T}$ |
|--------|----------------|---------------------------------|---------------------------------|-------------------------|
| 298.15 | 7.70 | 0 | 0.00 | 6.59 |
| 400 | 8.82 | 858 | 2.46 | 6.90 |
| 500 | 9.54 | 1776 | 4.51 | 7.55 |
| 600 | 10.11 | 2747 | 6.27 | 8.28 |
| 700 | 10.60 | 3722 | 7.86 | 9.06 |
| 800 | 11.04 | 4852 | 9.30 | 9.82 |
| 900 | 11.45 | 5978 | 10.63 | 10.58 |
| 1000 | 11.80 | 7143 | 11.85 | 11.30 |
| 1100 | 12.04 | 8336 | 12.99 | 12.00 |
| 1200 | 12.33 | 9556 | 14.05 | 12.68 |
| 1300 | 12.53 | 10804 | 15.04 | 13.32 |
| 1400 | 12.70 | 12071 | 15.98 | 13.95 |
| 1500 | 12.86 | 13357 | 16.87 | 14.56 |
| 1600 | 12.98 | 14651 | 17.71 | 15.14 |
| 1700 | 13.10 | 15954 | 18.50 | 15.71 |
| 1800 | 13.20 | 17267 | 19.25 | 16.25 |
| 1900 | 13.28 | 18590 | 19.97 | 16.78 |
| 2000 | 13.36 | 19921 | 20.65 | 17.28 |

Alekseev and Schvartsman^(42, 43)

studied the equilibria $V_2C-H_2-CH_4-V$ and $V_4C_3-V_2C-H_2-CH_4$ over the temperature interval 973 - 1273°K. Using the Gibbs free energy of formation of CH₄ reported by Richardson⁽⁴⁴⁾, they derived $\Delta G_{f, V_2C} = -11,500 - 0.49T$ and $\Delta G_{f, VC_{0.75}} = -10,800 - 1.1T$. These values are much less exothermic than expected when compared with the direct calorimetric value of VC_{0.87} and with the heats of formation of NbC and TaC where the data are well-established. The reason for the discrepancy between the equilibrium and calorimetric data are not understood.

It is worthwhile to point out that vanadium carbides are known to form solid solutions with vanadium nitrides⁽⁴⁵⁾ and with vanadium oxides⁽⁴⁶⁾, and one suspects that vanadium carbides may also take hydrogen into solution. The presence of hydrogen will complicate the analysis of the equilibrium measurements.

Rudy⁽⁴⁷⁾ evaluated the ternary phase diagrams V-Mo-C and V-W-C thermodynamically and obtained the following thermodynamic information:

$$\Delta G_{f, \text{MoC}_{1/2}} - \Delta G_{f, \text{VC}_{1/2}} = 4600 \pm 350 \text{ cal at } 1800^\circ\text{K}$$

$$\Delta G_{f, \text{WC}_{1/2}} - \Delta G_{f, \text{VC}_{1/2}} = 7500 \pm 300 \text{ cal at } 1750^\circ\text{K}$$

$$\Delta G_{f, \text{MoC}} - \Delta G_{f, \text{VC}} = 11,900 \text{ cal at } 2000^\circ\text{K}$$

and $\Delta G_{f, \text{WC}} - \Delta G_{f, \text{VC}} = 13,200 \pm 650 \text{ cal at } 2050^\circ\text{K}$

All the above MeC and Me₂C phases refer to metal-rich compositions.

(5) Vapor Pressure Data

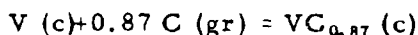
Fujishiro and Gokcen⁽⁴⁸⁾ measured the vapor pressure of vanadium over VC and graphite over the temperature interval 2346 - 2545°K using the Knudsen technique. The Third Law evaluation of their data yielded $\Delta H_{f, \text{st}} = -22,700 \pm 5000 \text{ cal/g-atom V}$. Since the weight loss of the empty Knudsen cell in their experiment was large in comparison to the actual weight loss of the sample, their results are viewed with doubt.

(6) Calorimetric Data

Mah⁽⁴⁹⁾ determined the heat of formation of VC by combustion calorimetry. The sample used by Mah was prepared by carbon reduction of vanadium pentoxide at 1000 - 1100°C. Chemical analysis of the prepared sample showed 80.22 % V, 18.32% C and 0.28% insoluble material. According to the author, the sample consisted of 96.02% VC, 3.7% V₂O₃ and 0.28% inert material. As discussed earlier, the VC phase extends to VC_{0.88} only, and therefore the sample must also have contained free graphite. From the combustion calorimetry, Mah obtained a value of $-24,350 \pm 400$ cal/g-atom V.

(7) Selection of Enthalpy and Free Energy Data

The heat of formation of VC_{0.87} at 298.15°K was selected to be $-24,350 \pm 2000$ cal/g-atom V based on the calorimetric value of Mah. With the selected value of $\Delta H_{f, st}$ for VC_{0.87}, and the available free energy functions of VC_{0.87}, vanadium, and graphite, the Gibbs free energy of formation of VC_{0.87} was calculated. The calculated ΔG_f values as a function of temperature were fitted to a linear equation and this equation is:



$$\Delta G_{f, 298.15 - 2000^\circ K} = -24,300 + 1.44 T$$

b. Niobium-Carbon System

(1) Phase Diagram

The phase diagram as shown in Figure 5 is based on the work of Storms and Krikorian⁽⁵¹⁾. However, preliminary experimental investigation of this system in our own laboratory

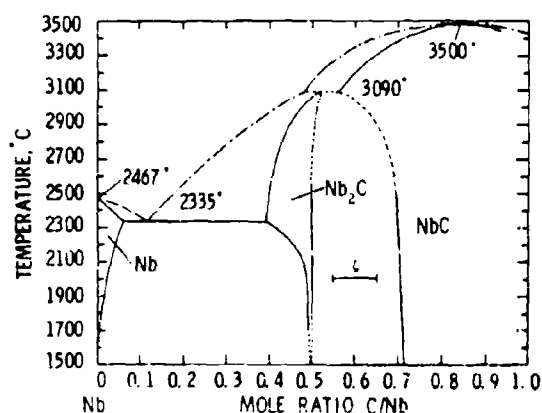


Figure 5. The Phase Diagram of the System Niobium-Carbon

indicates that the high-temperature phase relationships are much more complicated than this phase diagram suggests. In fact, the phase diagram is anticipated to be similar to that of the tantalum-carbon system which has been firmly established by us and which will be discussed in the section on Tantalum-Carbon System.

(2) Low-Temperature Data

Pankratz, Weller, and Kelley⁽⁵²⁾

measured the low temperature heat capacity of $\text{NbC}_{1.0}$ over the temperature interval 51.96 - 296.1°K. The sample used was supplied by the Union Carbide Corporation. Analysis of the sample showed 88.17% Nb, 11.74% total C, 0.39% free C, <0.05% N, 0.03% O, 0.02% Ti, 0.006% Ag and 0.002% Mn. Integration of the values of the heat capacity after correcting for the presence of 0.39% free carbon yielded the value of $S_{\text{st}} = 8.46 \pm 0.05$ cal/deg g-atom Nb. Using the available entropy of niobium⁽¹⁾ and of graphite⁽⁴⁾, $\Delta S_{\text{f, st}} = -1.60 \pm 0.1$ cal/deg g-atom Nb was obtained.

(3) High-Temperature Data

The high-temperature values selected for $\text{NbC}_{1.0}$ were based on the heat content of Pankratz, Weller and Kelley⁽⁵²⁾ over the temperature interval 398.5 - 1802.3°K; of Gel'd and Kussenko⁽⁵³⁾ over the temperature interval 298 - 1800°K; and of Levinson⁽⁵⁴⁾ over the temperature interval 1289 - 2778°K. The selected values also join smoothly with the low-temperature heat capacity. The data of Pankratz, et.al. scatter less than $\pm 0.5\%$ about the selected curve. From 1300 to 1800°K, the data of Levinson are lower than the selected values by as much as 2%. Above 1800°K the data of Levinson joins smoothly with the data of Pankratz, et.al.; and with those of Gel'd and Kussenko to form the selected curve with a scatter of $\pm 1\%$.

From 600 to 670°K, the data of Pankratz, et.al. showed a small anomaly whose origin is not known. For

convenience the authors treated this anomaly as an isothermal transformation at 630°K with a small heat effect of 40 cal/g-atom Nb. For lack of other evidence to support this phenomenon, and because of the fact that the heat effect is a small quantity, we have assumed that NbC does not go through a phase transformation at 670°K.

Based on the selected values of ΔH_f° and S_{st}° , the calculated high-temperature thermal properties of $\text{NbC}_{\sim 1.0}$ are reported in Table 4. The tabulated heat content of $\text{NbC}_{\sim 1.0}$ over the temperature interval 298.15 - 3000°K may be represented by the following analytical expression with an average standard deviation of 13 cal/g-atom Nb, and with a maximum deviation of 50 cal/g-atom Nb at 3000°K:

$$H_T - H_{st} = 11.366 T + 0.55871 \times 10^{-3} T^2 + 2.6854 \times 10^5 T^{-1} - 4340.1$$

Gel'd and Kussenko⁽⁵³⁾ also measured the heat contents of $\text{NbC}_{0.867}$, $\text{NbC}_{0.749}$, and $\text{NbC}_{0.50}$ over the temperature interval 298 - 1800°K, and gave the following equations to represent their data:

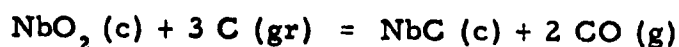
$$\begin{array}{ll} \text{NbC}_{0.867} & H_T - H_{st} = 9.70 T + 0.995 \times 10^{-3} T^2 + 1.51 \times 10^5 T^{-1} - 3485 \\ \text{NbC}_{0.749} & H_T - H_{st} = 8.95 T + 1.127 \times 10^{-3} T^2 + 1.26 \times 10^5 T^{-1} - 3190 \\ \text{NbC}_{0.50} & H_T - H_{st} = 7.94 T + 0.750 \times 10^{-3} T^2 + 1.025 \times 10^5 T^{-1} - 2776 \end{array}$$

(4) Reaction Equilibrium Data

Worrell and Chipman⁽⁴¹⁾ studied the equilibrium $\text{NbO}_2\text{-C-NbC-CO}$ over the temperature interval 1175 - 1261°K, and obtained $\Delta G_R = 100,400 - 80.3 T$ for the reaction:

Table 4. High-Temperature Thermal Properties of NbC_{~1.0}

| T°K | C _p | H _T -H _{st} | S _T -S _{st} | $-\frac{G_T-H_{st}}{T}$ | ΔC _p |
|--------|----------------|---------------------------------|---------------------------------|-------------------------|-----------------|
| 298.15 | 8.82 | 0 | 0.00 | 8.46 | 0.90 |
| 400 | 10.05 | 966 | 2.78 | 8.82 | 1.14 |
| 500 | 10.78 | 2009 | 5.10 | 9.54 | 1.12 |
| 600 | 11.33 | 3117 | 7.12 | 10.39 | 1.05 |
| 700 | 11.66 | 4266 | 8.89 | 11.26 | 0.88 |
| 800 | 11.90 | 5445 | 10.47 | 12.12 | 0.72 |
| 900 | 12.07 | 6643 | 11.88 | 12.96 | 0.57 |
| 1000 | 12.22 | 7859 | 13.16 | 13.76 | 0.44 |
| 1100 | 12.38 | 9088 | 14.33 | 14.53 | 0.36 |
| 1200 | 12.52 | 10332 | 15.41 | 15.26 | 0.27 |
| 1300 | 12.66 | 11591 | 16.42 | 15.96 | 0.21 |
| 1400 | 12.79 | 12862 | 17.36 | 16.63 | 0.17 |
| 1500 | 12.92 | 14146 | 18.25 | 17.28 | 0.14 |
| 1600 | 13.04 | 15450 | 19.09 | 17.89 | 0.12 |
| 1700 | 13.16 | 16766 | 19.89 | 18.48 | 0.09 |
| 1800 | 13.26 | 18091 | 20.64 | 19.05 | 0.06 |
| 1900 | 13.38 | 19426 | 21.36 | 19.60 | 0.05 |
| 2000 | 13.50 | 20766 | 22.05 | 20.13 | 0.04 |
| 2100 | 13.61 | 22116 | 22.71 | 20.64 | 0.04 |
| 2200 | 13.73 | 23480 | 23.35 | 21.13 | 0.04 |
| 2300 | 13.86 | 24857 | 23.96 | 21.61 | 0.04 |
| 2400 | 13.98 | 26250 | 24.55 | 22.07 | 0.05 |
| 2500 | 14.12 | 27655 | 25.12 | 22.52 | 0.08 |
| 2600 | 14.27 | 29082 | 25.68 | 22.96 | 0.12 |
| 2700 | 14.42 | 30523 | 26.23 | 23.38 | 0.15 |
| 2740 | 14.48 | 31109 | 26.44 | 23.55 | |
| 2800 | 14.58 | 31974 | 26.75 | 23.80 | |
| 2900 | 14.76 | 33442 | 27.27 | 24.20 | |
| 3000 | 14.94 | 34927 | 27.77 | 24.59 | |



Using the free energy of formation equations for NbO_2 ⁽⁵⁵⁾ and CO ⁽⁹⁾,

Worrell and Chipman obtained the following expression for the free energy of formation of $\text{NbC}_{1.0}$ over the temperature interval 1175 - 1261°K:

$\Delta G_f = -31,100 + 0.4 \text{ T cal/g-atom Nb}$. From the ΔG_f equation for $\text{NbC}_{1.0}$, and from the available thermal data, one obtained

$$\Delta H_{f, \text{st}} = -31,800 \pm 900 \text{ cal/g-atom Nb}$$

for $\text{NbC}_{1.0}$

Rudy⁽⁴⁷⁾ evaluated the Mo-Nb-C phase diagram thermodynamically at 2170°K, and obtained $\Delta G_{z, 2170^\circ\text{K}} = 710(\pm 70) \text{ cal}$ for the following reaction:



(5) Vapor Pressure Data

Fries⁽⁵⁶⁾ studied the Langmuir vaporization of NbC_x over the temperature interval 2260 - 2940°K. He found that NbC_x lost carbon preferentially down to $\text{NbC}_{0.75}$, at which composition the vaporization proceeds congruently at 2940°K.

(6) Calorimetric Data

The heats of formation of both the NbC and Nb_2C phases have been determined using the combustion calorimetry by Mah and Boyle⁽²⁶⁾; Huber, Head, Holley, Storms, and Krikorian⁽⁵⁷⁾; Kornikov, Leonidov, and Skuratov⁽⁵⁸⁾; and Kussenko and Gel'd⁽⁵⁹⁾. The results obtained by the various investigators are summarized below:

| <u>Investigator</u> | <u>Atomic Ratio, C/Nb</u> | <u>$\Delta H_{f, st}$, cal/g-atom Nb</u> |
|---------------------|---------------------------|---|
| Mah and Boyle | 0.9445 | - 31,750 \pm 800 |
| Huber, et.al. | 0.489 - 0.984 | See Figure 6 |
| Kornikov, et.al. | 0.931 | - 31,000 \pm 600 |
| Kussenko and Gel'd | 0.74 - 0.98 | See Text |

The sample used by Mah and Boyle was prepared by direct combination in vacuum at a temperature of 2300 - 2400°C. Chemical analysis of the sample showed 10.82% C, 89.10% Nb, and 0.08% unaccounted impurities which were attributed to oxygen and nitrogen. The maximum impurities in any of the samples used by Huber, et.al. were < 0.1% N, < 0.18% O, < 0.047% H, and < 0.03% Fe. The heats of formation reported by Kussenko and Gel'd were about 1000 to 2000 cal/g-atom Nb more exothermic than the values obtained by Huber, et.al. According to Storms⁽¹⁵⁾, the values reported by Kussenko and Gel'd may be in error because of the presence of large amounts of oxygen in their sample.

(7) Selection of Enthalpy and Free Energy Data

The selected heats of formation of the NbC and the Nb₂C phases at 298.15°K as a function of composition were based on the calorimetric values of Huber, et.al.; Mah and Boyle; and Kornikov, et.al.; and the value derived from the equilibrium measurements of Worrell and Chipman, as shown in Figure 6. The selected values are:

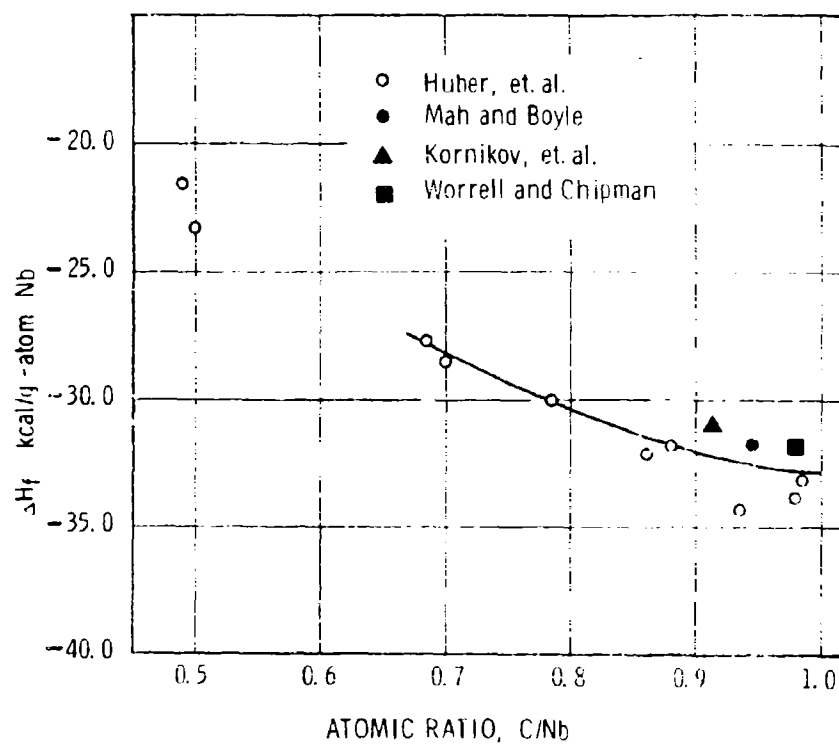
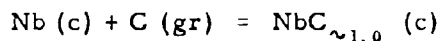


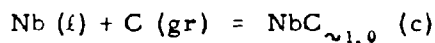
Figure 6. The Heats of Formation of the Niobium Monocarbide and Subcarbide

| Atomic Ratio C/Nb | $\Delta H_{f, st}$, cal/g-atom Nb |
|-------------------|------------------------------------|
| ~ 1.00 | $- 32,800 \pm 1200$ |
| 0.90 | $- 32,000$ |
| 0.80 | $- 30,500$ |
| 0.70 | $- 28,200$ |
| 0.50 | $- 22,500 \pm 1700$ |

Using the selected value of $\Delta H_{f, st}$ for $NbC_{\sim 1.0}$, and the available free energy functions for $NbC_{\sim 1.0}$, $Nb^{(1)}$, and $C^{(4)}$; the Gibbs free energy of formation of $NbC_{\sim 1.0}$ as a function of temperature was calculated. The calculated values of ΔG_f as a function of temperature were fitted to two linear equations. These equations are:



$$\Delta G_{f, 298.15 - 2740^\circ K} = - 32,190 + 0.39 T$$



$$\Delta G_{f, 2740 - 3000^\circ K} = - 38,380 + 2.65 T$$

c. Tantalum-Carbon System

(1) Phase-Diagram

The phase diagram as shown in Figure 7 is based on the recent work of Rudy, Brukl, and Harmon⁽⁶⁰⁾. Both the α - Ta_2C and β - Ta_2C phases have the same arrangement of the

metal lattice, i.e. hexagonal close-packed, but the structure of the metastable ζ -phase has not yet been determined.

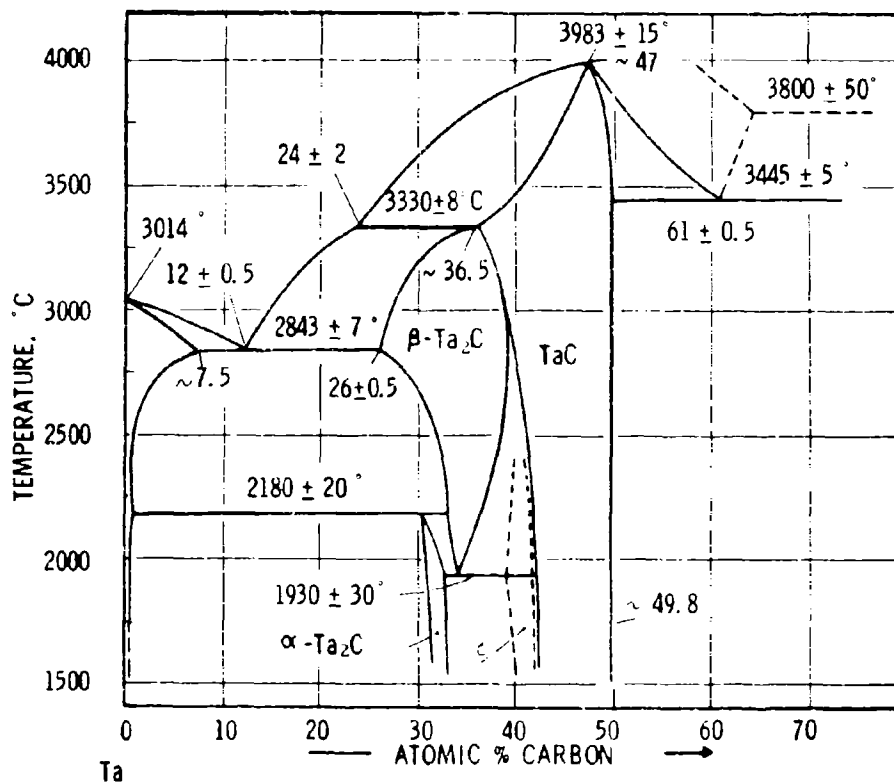


Figure 7. The Phase Diagram of the Tantalum-Carbon System

(2) Low-Temperature Data

Kelley⁽⁶¹⁾ measured the low-temperature heat capacity of TaC over the temperature interval 54 - 295°K. The sample used was supplied by Fansteel Metallurgical Co., and chemical analysis of the sample showed 4.26% C and 0.02% impurities. Integration of the heat capacity yielded the value of $S_{st} = 10.1 \pm 0.1$ cal/deg g-atom Ta

for $\text{TaC}_{\sim 1.0}$. Using the available entropy data of Ta⁽¹⁾ and of graphite⁽⁴⁾, $\Delta S_{f, st} = -1.18 \pm 0.15$ cal/deg g-atom Ta was obtained.

(3) High-Temperature Data

The high-temperature values selected for $\text{TaC}_{\sim 1.0}$ were based on the heat content measurement of Levinson⁽⁵⁴⁾ over the temperature interval 1296 - 2843°K and the value of C_p at 298.15°K reported by Kelley⁽⁶⁾. The heat content data of Mezaki, Jambois, Gangopadhy, and Margrave⁽²⁰⁾ over the temperature interval 476 - 1113°K were higher than our selected value. At 1113°K, the value of Y as reported by Mezaki, et.al. was about 10% higher. We believe the data of Mezaki, et.al. are in error since the extrapolation of their data to higher temperature would lead to rather large C_p values.

The calculated high-temperature thermal properties of $\text{TaC}_{\sim 1.0}$, based on the selected values of Y and S_{st} , are reported in Table 5. The tabulated content of $\text{TaC}_{\sim 1.0}$ over the temperature interval 298.15 - 1800°K may be represented by the following analytical expression with an average standard deviation of 3 cal/g-atom Ta, and a maximum deviation of 7 cal/g-atom Ta at 1800°K:

$$H_T - H_{st} = 10.322 T + 1.0368 \times 10^{-3} T^2 + 1.8902 \times 10^{-5} T^3 - 3803.4$$

From 1800°K to 3000°K, the heat content of $\text{TaC}_{\sim 1.0}$ may be represented by the analytical expression below with an average standard deviation of 7 cal/g-atom Ta, and a maximum deviation of 12 cal/g-atom Ta at 2100°K:

$$H_T - H_{st} = 20.144 T + 0.83838 \times 10^{-3} T^2 + 98.683 \times 10^{-5} T^3 - 2077.5$$

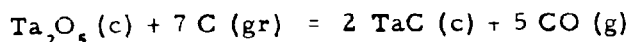
Table 5. High-Temperature Thermal Properties of $\text{TaC}_{\sim 1.0}$

| T°K | C_p | $H_T - H_{st}$ | $S_T - S_{st}$ | $-\frac{G_T - H_{st}}{T}$ | ΔC_p |
|--------|-------|----------------|----------------|---------------------------|--------------|
| 298.15 | 8.79 | 0 | 0.00 | 10.11 | 0.69 |
| 400 | 9.93 | 967 | 2.78 | 10.47 | 0.86 |
| 500 | 10.58 | 1998 | 5.08 | 11.19 | 0.78 |
| 600 | 11.03 | 3076 | 7.04 | 12.03 | 0.66 |
| 700 | 11.39 | 4195 | 8.77 | 12.88 | 0.56 |
| 800 | 11.69 | 5350 | 10.31 | 13.73 | 0.50 |
| 900 | 11.96 | 6576 | 11.71 | 14.55 | 0.48 |
| 1000 | 12.22 | 7748 | 12.98 | 15.34 | 0.50 |
| 1100 | 12.46 | 8981 | 14.16 | 16.10 | 0.53 |
| 1200 | 12.71 | 10236 | 15.25 | 16.83 | 0.59 |
| 1300 | 12.94 | 11511 | 16.27 | 17.52 | 0.66 |
| 1400 | 13.16 | 12815 | 17.24 | 18.19 | 0.74 |
| 1500 | 13.39 | 14134 | 18.15 | 18.83 | 0.85 |
| 1600 | 13.58 | 15479 | 19.01 | 19.45 | 0.93 |
| 1700 | 13.76 | 16850 | 19.85 | 20.04 | 1.00 |
| 1800 | 13.93 | 18247 | 20.64 | 20.64 | 1.08 |
| 1900 | 14.07 | 19671 | 21.41 | 21.17 | 1.12 |
| 2000 | 14.19 | 21086 | 22.14 | 21.71 | 1.15 |
| 2100 | 14.28 | 22541 | 22.85 | 22.23 | 1.16 |
| 2200 | 14.34 | 23963 | 23.51 | 22.73 | 1.15 |
| 2300 | 14.37 | 25403 | 24.15 | 23.22 | 1.09 |
| 2400 | 14.40 | 26853 | 24.77 | 23.69 | 1.04 |
| 2500 | 14.42 | 28303 | 25.36 | 24.15 | 0.99 |
| 3000 | 14.42 | 35400 | 27.95 | 26.26 | 0.60 |

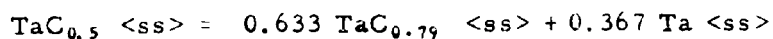
(4) Reaction Equilibrium Data

Worrell and Chipman⁽⁴¹⁾ studied

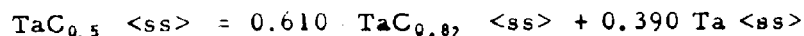
the equilibrium $\text{Ta}_2\text{O}_5\text{-C-TaC-CO}$ over the temperature interval 1265 - 1366°K. The Third Law treatment of their data using the available free energy functions for $\text{CO}^{(4)}$, TaC , $\text{C}^{(4)}$, and $\text{Ta}_2\text{O}_5^{(50,62)}$ yielded $\Delta H_{R, st} = 286,1100 \pm 750$ cal for the following reaction:



The uncertainty assigned to $\Delta H_{R, st}$ only takes account of the scatter in the vapor pressure data of CO. Using the available values of $\Delta H_{f, st}$ for $\text{CO}^{(4)}$ and $\text{Ta}_2\text{O}_5^{(63)}$, the heat of formation of $\text{TaC}_{\sim 1.0}$ was calculated to be $-35,300 \pm 1400$ cal/g-atom Ta. Thermodynamic evaluation of the Ta-W-C phase diagram at 1963°K by Rudy⁽⁴⁷⁾ yielded $\Delta G_{Z, 1973^\circ K} = 2100$ cal for the following reaction:



Similar thermodynamic evaluation of Hf-Ta-C phase diagram by Rudy and Nowotny⁽³⁶⁾ at 2123°K yielded $\Delta G_{Z, 2123^\circ K} = 2500$ cal for the reaction:



These two values of ΔG_Z are in reasonable agreement.

(5) Vapor Pressure Data

Hoch, Blackburn Dingley, and Johnston⁽⁶⁴⁾ measured the vapor pressure of graphite in equilibrium with TaC over the temperature interval 2275 - 3265°K. Since the carbon

component at the carbon-rich boundary of the TaC phase is in equilibrium with pure graphite, they essentially measured the vapor pressure of graphite.

(6) Calorimetric Data

The heats of formation of both the TaC and Ta₂C phases have been determined using combustion calorimetry by Humphrey⁽⁶³⁾; Mah⁽⁶⁵⁾; Huber, Head, Holley, and Bowman⁽⁶⁶⁾; Kornikov, Leonidov, and Skuratov⁽⁵⁸⁾; and Smirnova and Ormont⁽⁶⁷⁾. The results obtained by the various investigators are summarized below:

| <u>Investigator</u> | <u>Atomic Ratio, C/Ta</u> | <u>$\Delta H_{f, st}$, cal/g-atom Ta</u> |
|---------------------|---------------------------|---|
| Humphrey | ~ 1.0 | $- 38,500 \pm 600$ |
| Mah | ~ 1.0 | $- 35,270 \pm 700$ |
| Huber, et.al. | 0.485 - 0.998 | See Figure 8 |
| Kornikov, et.al. | 0.982 | $- 33,700 \pm 1000$ |
| Smirnova and Ormont | 0.60 - 0.90 | See text |

The sample used by Humphrey contained the following impurities: 0.27% Nb, 0.10% Ti, 0.05% Si, 0.01% Fe, and 0.01% Zr. On the other hand, Mah used a rather pure sample which was 99.977% TaC, 0.1% TaO, 0.1% TaN, and 0.1% free carbon. The discrepancy between these two values is undoubtedly caused by the presence of impurities in the sample used by Humphrey. The maximum impurities present in any of the samples used by Huber, et.al. were: < 0.12% free C, < 0.21% N, < 0.023% O, < 0.029% H, < 0.12% Nb, and < 0.02% W.

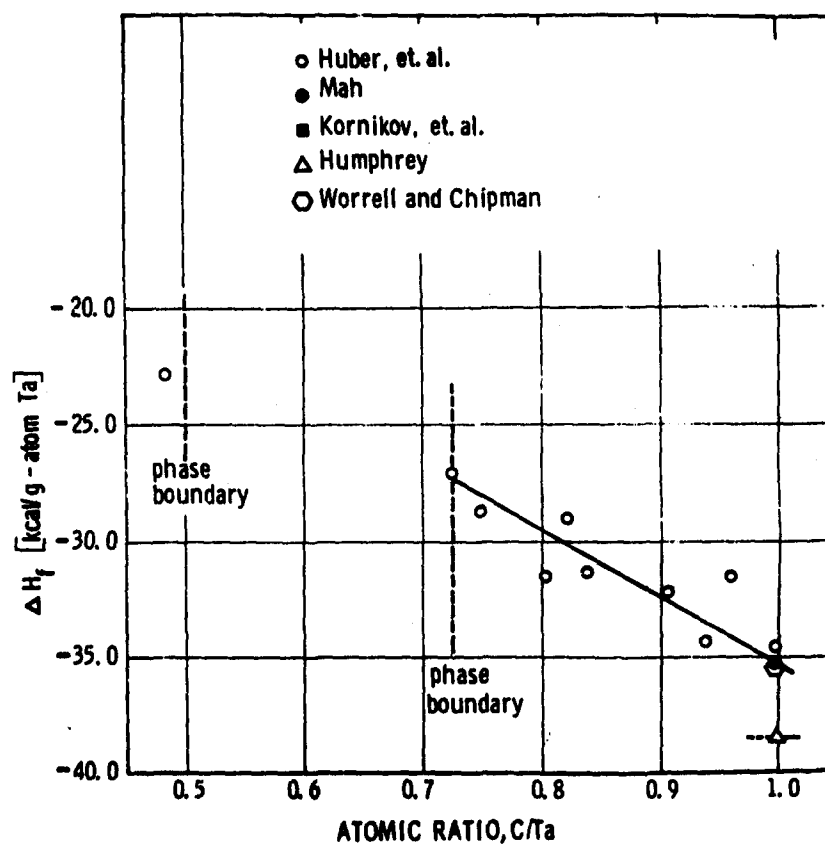


Figure 8. The heats of Formation of the TaC and Ta₂C Phases

The heat of formation of the TaC phase reported by Smirnova and Ormont was about a few kilocalories less exothermic than the values of Huber, et.al. The discrepancy is probably due to the inhomogeneous alloys used by Smirnova and Ormont as pointed out by Huber, et.al. in their paper.

(7) Selection of Enthalpy and Free Energy Data

The heats of formation of both the TaC and Ta₂C phases at 298.15°K as a function of composition were selected based on the calorimetric values of Mah, Huber, et.al., and Kornikov, et.al., and the value derived from the equilibrium measurement of Worrell and Chipman, as shown in Figure 8. The selected values are:

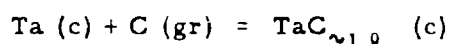
| <u>Atomic Ratio, C Ta</u> | <u>$\Delta H_{f, st}$, cal/g-atom Ta</u> |
|---------------------------|---|
| ~ 1.0 | - 35,050 \pm 1000 |
| 0.900 | - 32,500 |
| 0.800 | - 29,500 |
| 0.725 | - 27,400 |
| 0.485 | - 22,900 \pm 1700 |

The selected values of $\Delta H_{f, st}$ for the TaC phase may be represented by the following analytical expression:

$$\Delta H_{f, st} = -6,840 - 28,260 x \text{ in cal/g-atom Ta}$$

where x is the atomic ratio, C Ta.

With this selected value of $\Delta H_{f, st}$ for $TaC_{\sim 1.0}$, and the available free energy functions for TaC , $C^{(4)}$, and $Ta^{(1)}$, the Gibbs free energy of formation of $TaC_{\sim 1.0}$ as a function of temperature was calculated. The calculated ΔG_f values as a function of temperature may be represented by the following analytical expression:



$$\Delta G_{f, 298.15 - 3000^\circ K} = -35,335 - 1.7949 T \log T + 6.4757 T$$

3. Group VI Metal Carbon Systems

In addition to the $\alpha\text{-Me}_2C$, $\beta\text{-Me}_2C$, and MeC phases, new phases appear in the Mo-C and the W-C systems at high temperatures, but in the Cr-C system there appear three intermediate phases whose structures are rather different from the phases in the other carbide systems. In contrast to the thermodynamic behavior of the group IV and V carbides, the heats of formation of all the group VI carbides are relatively small quantities, and consequently the stabilities of these carbide phases at high temperatures are strongly influenced by the entropy term.

a. Chromium-Carbon System

(1) Phase Diagram

The phase diagram of the chromium-carbon system as shown in Figure 9 is based on the work of Bloom and Grant⁽⁶⁸⁾. The three intermediate phases are $Cr_{23}C_6$, which is complex f.c.c. with 116 atoms per unit cell ($D8_4$ type); Cr_7C_3 , which is hexagonal with 80 atoms per unit cell; and Cr_3C_2 , which is orthorhombic with 20 atoms per unit cell ($D5_{10}$ type).

(2) Low-Temperature Data

Kelley, Boericke, Moore, Huffman,
and Bangert⁽⁶⁹⁾ measured the low-temperature heat capacities of $\text{CrC}_{2/3}$

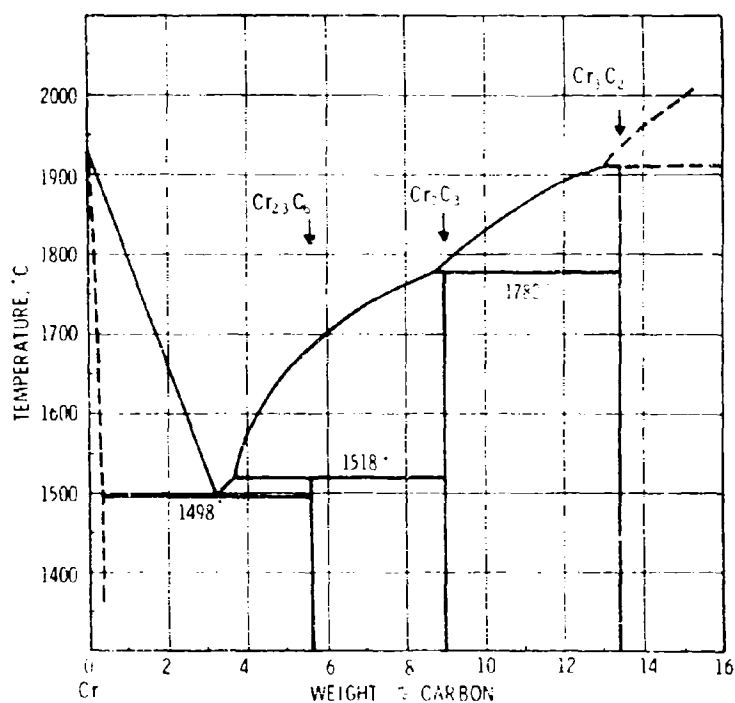


Figure 9. The Phase Diagram of Chromium-Carbon System

$\text{CrC}_{3/7}$, and $\text{CrC}_{6/23}$ over the temperature interval 53 - 296°K. The low-temperature heat capacity of $\text{CrC}_{2/3}$ over the temperature interval 12 - 301°K was also determined by DeSorbo⁽⁷⁰⁾. All these data were evaluated by Kelley and King⁽⁶²⁾. Integration of the heat capacities by Kelley and King yielded the values of $S_{\text{st}} = 6.81 \pm 0.03$, 6.86 ± 0.04 , and 6.34 ± 0.03 cal/deg g-atom Cr for the three chromium carbides,

$\text{CrC}_{2/3}$, $\text{CrC}_{3/7}$, and $\text{CrC}_{6/23}$. Using the available values of S_{st} for chromium⁽⁶²⁾ and graphite⁽⁴⁾, $\Delta S_{f, \text{st}} = 0.22 \pm 0.08$, 0.59 ± 0.08 and 0.30 ± 0.07 cal/deg g-atom Cr for the three chromium carbides, were obtained.

(3) High-Temperature Data

Kelley, et.al.⁽⁶⁹⁾ also measured the high-temperature heat contents of $\text{CrC}_{2/3}$ over the temperature interval 298 - 1576°K, of $\text{CrC}_{3/7}$ over the temperature interval 298 - 1578°K, and of $\text{CrC}_{6/23}$ over the temperature interval 298 - 1578°K. Oriani and Murphy⁽⁷¹⁾ measured the heat content of $\text{CrC}_{2/3}$ over the temperature interval 273 - 1188°K. All these data were evaluated by Kelley⁽⁵⁰⁾ and the heat and entropy increments above 298.15°K were calculated. Based on the heat content values selected by Kelley⁽⁵⁰⁾, the high-temperature thermal properties of $\text{CrC}_{2/3}$, $\text{CrC}_{3/7}$, and $\text{CrC}_{6/23}$, all expressed per g-atom Cr, are reported in Tables 6, 7, and 8. The heat content of $\text{CrC}_{2/3}$ over the range 298 - 1600°K, of $\text{CrC}_{3/7}$ over the range 298 - 1500°K, and of $\text{CrC}_{6/23}$ over the range 298.15 - 1800°K, as reported in Tables 6, 7, and 8 may be represented by the following three analytical expressions:

$$H_T - H_{\text{st}} = 10.01 T + 0.930 \times 10^{-3} T^2 + 2.47 \times 10^{-5} T^{-1} - 3894$$

$$H_T - H_{\text{st}} = 8.137 T + 1.04 \times 10^{-3} T^2 + 1.45 \times 10^{-5} T^{-1} - 3003$$

$$H_T - H_{\text{st}} = 7.355 T + 0.920 \times 10^{-3} T^2 + 1.26 \times 10^{-5} T^{-1} - 2697$$

(4) Reaction Equilibrium Data

In addition to measuring both the low-temperature and high-temperature thermal properties of $\text{CrC}_{2/3}$, $\text{CrC}_{3/7}$,

Table 6. High-Temperature Thermal Properties of $\text{CrC}_{2/3}$

| T°K | C_p | $H_T - H_{st}$ | $S_T - S_{st}$ | $-\frac{G_T - H_{st}}{T}$ |
|--------|-------|----------------|----------------|---------------------------|
| 298.15 | 7.84 | 0 | 0 | 6.81 |
| 400 | 9.14 | 873 | 2.51 | 7.14 |
| 500 | 9.91 | 1840 | 4.67 | 7.80 |
| 600 | 10.43 | 2867 | 6.54 | 8.57 |
| 700 | 10.82 | 3927 | 8.17 | 9.37 |
| 800 | 11.13 | 5020 | 9.63 | 10.16 |
| 900 | 11.40 | 6140 | 10.95 | 10.94 |
| 1000 | 11.64 | 7287 | 12.16 | 11.68 |
| 1100 | 11.85 | 8463 | 13.28 | 12.40 |
| 1200 | 12.05 | 9663 | 14.32 | 13.08 |
| 1300 | 12.23 | 10880 | 15.29 | 13.73 |
| 1400 | 12.38 | 12110 | 16.21 | 14.37 |
| 1500 | 12.52 | 13357 | 17.07 | 14.98 |
| 1600 | 12.65 | 14617 | 17.88 | 15.55 |

Table 7. High-Temperature Thermal Properties of $\text{CrC}_{3/7}$

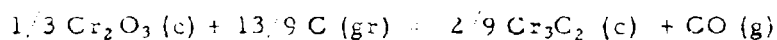
| T°K | C_p | $H_T - H_{st}$ | $S_T - S_{st}$ | $-\frac{G_T - H_{st}}{T}$ |
|--------|-------|----------------|----------------|---------------------------|
| 298.15 | 7.13 | 0 | 0 | 6.86 |
| 400 | 8.00 | 777 | 2.24 | 7.16 |
| 500 | 8.55 | 1617 | 4.11 | 7.74 |
| 600 | 8.97 | 2493 | 5.71 | 8.41 |
| 700 | 9.33 | 3408 | 7.12 | 9.11 |
| 800 | 9.62 | 4354 | 8.38 | 9.80 |
| 900 | 9.88 | 5320 | 9.51 | 10.46 |
| 1000 | 10.10 | 6318 | 10.57 | 11.11 |
| 1100 | 10.31 | 7337 | 11.54 | 11.73 |
| 1200 | 10.53 | 8371 | 12.44 | 12.32 |
| 1300 | 10.74 | 9428 | 13.28 | 12.89 |
| 1400 | 10.95 | 10528 | 14.10 | 13.44 |
| 1500 | 11.16 | 11678 | 14.89 | 13.96 |

Table 8. High-Temperature Thermal Properties of $\text{CrC}_{6/23}$

| $T^\circ\text{K}$ | C_p | $H_T - H_{st}$ | $S_T - S_{st}$ | $-\frac{G_T - H_{st}}{T}$ |
|-------------------|-------|----------------|----------------|---------------------------|
| 298.15 | 6.49 | 0 | 0.00 | 6.34 |
| 400 | 7.19 | 702 | 2.02 | 6.60 |
| 500 | 7.69 | 1465 | 3.73 | 7.14 |
| 600 | 8.07 | 2259 | 5.17 | 7.74 |
| 700 | 8.39 | 3080 | 6.43 | 8.37 |
| 800 | 8.65 | 3935 | 7.57 | 8.99 |
| 900 | 8.89 | 4811 | 8.60 | 9.59 |
| 1000 | 9.13 | 5706 | 9.55 | 10.18 |
| 1100 | 9.36 | 6622 | 10.42 | 10.74 |
| 1200 | 9.60 | 7559 | 11.23 | 11.27 |
| 1300 | 9.83 | 8520 | 12.00 | 11.79 |
| 1400 | 10.06 | 9511 | 12.74 | 12.29 |
| 1500 | 10.30 | 10528 | 13.44 | 12.76 |
| 1600 | 10.53 | 11572 | 14.12 | 13.23 |
| 1700 | 10.77 | 12646 | 14.77 | 13.67 |
| 1800 | 11.00 | 13746 | 15.40 | 14.10 |

and CrC_6 ; Kelley, et.al.⁽⁶⁹⁾ also studied the following four equilibria: Cr_2O_3 - Cr_3C_2 -C-CO over the temperature interval 1243 - 1381°K, Cr_2O_3 - Cr_7C_3 - Cr_3C_2 -CO over the temperature interval 1306 - 1495°K, Cr_2O_3 - Cr_{23}C_6 - Cr_7C_3 -CO over the temperature interval 1503 - 1721°K, and Cr_2O_3 -Cr- Cr_{23}C_6 -CO over the temperature interval 1601 - 1770°K. From these four equilibrium measurements and from the available thermal properties, Kelley, et.al.⁽⁶⁹⁾ derived a value of the heat of formation for Cr_2O_3 at 298.15°K which is about two kilocalories less exothermic than the recent calorimetric value reported by Mah⁽⁷²⁾. Based on this evidence, we suspect that the equilibrium measurements of Kelley, et.al. might be in error.

Using the available values of the free energy function for $\text{CrC}_{2/3}$ ^(50,62), Cr_2O_3 ^(50,62), C⁽⁴⁾, and CO⁽⁴⁾, the Third Law treatment of the data reported by Kelley, et.al. for the equilibrium Cr_2O_3 - Cr_3C_2 - C - O yielded a value of $\Delta H_{R, \text{st}} = 59,120$ cal/g-mole CO for the following reaction:



Using the heats of formation of Cr_2O_3 ⁽⁷²⁾ and CO⁽⁴⁾,

$$\Delta H_{f, \text{st}} = -24,140 \text{ cal/g-mole}$$

was obtained for Cr_3C_2 .

More recently, Gleiser⁽⁷³⁾ restudied the equilibrium Cr_2O_3 - Cr_3C_2 -C-CO over the temperature interval 1316 - 1366°K. A Third Law treatment of Gleiser's data yielded a value

of $\Delta H_{Rst} = 58,360 \pm 450$ cal/g-mole CO. From this value,

$$\Delta H_{f, st} = -27,550 \pm 2200 \text{ cal/g-mole}$$

was obtained for Cr_3C_2 , which we judge to be the more reliable one.

Rudy and Chang⁽⁷⁴⁾ evaluated the various equilibria existing in the ternary phase diagrams Mo-Cr-C and W-Cr-C at 1573°K thermodynamically and obtained the following values for the Gibbs free energies of reaction:

| <u>Reaction</u> | <u>$\Delta G_R, 1573^\circ K$</u> |
|--|--|
| (a) $CrC_{2/3} <ss> = CrC_{1/2} <ss, Mo_2C\text{-type}> + 1/6 C <ss>$ | 945 |
| (b) $CrC_{1/2} <ss, Mo_2C\text{-type}> = 0.7 CrC_{3/7} <ss>$ + $0.3 CrC_{2/3} <ss>$ | -270 ± 50 |
| (c) $CrC_{2/3} <ss> = 0.88 CrC_{0.45} <ss, Mo_2C\text{-type}>$ + $0.12 CrC_{6/23} <ss>$ | 350 ± 30 |
| (d) $CrC_{6/23} <ss> = 0.42 Cr <ss>$ + $0.58 CrC_{0.45} <ss, Mo_2C\text{-type}>$ | 915 ± 55 |

The fact that the values of ΔG_R obtained from the two different ternary phase diagrams agree with each other leads us to have confidence in the reliability of these values. Based on the values of the Gibbs free energy of formation of $CrC_{2/3}$ derived from Gleiser's data and the available thermal properties, the Gibbs free energy of formation for $CrC_{3/7}$ and $CrC_{6/23}$ will be obtained using the ΔG_R values for the four reactions (a), (b), (c), and (d) obtained by Rudy and Chang⁽⁷⁴⁾.

Alekseev and Shvartsman⁽⁴³⁾

studied the equilibrium $\text{Cr}_{23}\text{C}_6\text{-H}_2\text{-CH}_4\text{-Cr}$ over the temperature interval 973 - 1223°K. From this study, Alekseev and Shvartsman obtained

$\Delta G_f = -3550 - 0.05T$ cal/g-atom Cr for $\text{CrC}_{6/23}$. At 1100°K

$\Delta G_f = -3610$ cal/g-atom Cr which is about 2700 cal less exothermic than the selected value. The fact that Alekseev and Shvartsman obtained an apparent zero entropy of formation suggests that their data might be in error. The entropy of formation of $\text{CrC}_{6/23}$, according to the thermal data, is 0.89 cal/deg g-atom Cr at 1000°K.

(5) Vapor Pressure Data

Fujishiro and Gokcen⁽⁷⁵⁾ measured

the vapor pressure of Cr over Cr_3C_2 and graphite over the temperature interval 1908 - 2237°K by means of Knudsen technique. From their data, Fujishiro and Gokcen derived $\Delta H_{f, st} = -24,630$ cal/g-mole Cr_3C_2 , which is about three kcal less exothermic than the value derived from Gleiser's equilibrium data. Since the weight loss of the empty Knudsen cell in Fujishiro and Gokcen's experiments without orifice was comparable to the actual weight loss through the orifice, their data might be subject to large uncertainties. Moreover, their $\Delta H_{f, st}$ value was derived from the difference of two large heat of vaporization values.

⁽⁷⁶⁾
Vintaikin also studied the vaporiza-

tion of Cr_3C_2 over the temperature interval 1373 - 1573°K using the Knudsen technique. He obtained $\Delta G_f = -8,190 - 6.99T$ cal/g-mole Cr_3C_2 . At 1500°K, the value of ΔG_f obtained for Cr_3C_2 by Vintaikin is about 14 kcal less exothermic than the value derived from Gleiser's data. The fact that

Virtainkin obtained a rather large value for the apparent entropy of formation suggests that his data might be in error. The entropy of formation of Cr_3C_2 at 1500°K, according to thermal data, is 5.62 cal/deg g-mole Cr_3C_2 .

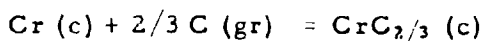
(6) Calorimetric Data

No calorimetric data was found in the literature for any of the three chromium carbides

(7) Selection of Enthalpy and Free Energy Data

a. $\text{CrC}_{2/3}$

The heat of formation of $\text{CrC}_{2/3}$ at 298.15°K was selected to be $-9,180 \pm 700$ cal/g-atom Cr based on the equilibrium data of Gleiser and the available free energy functions for $\text{CrC}_{2/3}$, Cr, and C. Based on this selected value of $\Delta H_{f, \text{st}}$, the Gibbs free energy of formation of $\text{CrC}_{2/3}$ as a function of temperature was calculated. The calculated ΔG_f values were fitted to the following linear equation:

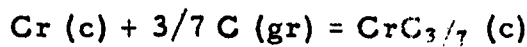


$$\Delta G_{f, 298.15 - 1600^\circ\text{K}} = -8,740 - 1.30T$$

b. $\text{CrC}_{3/7}$

Based on the selected values of ΔG_f for $\text{CrC}_{2/3}$ and the values of ΔG_R for reactions (a) and (b) reported by Rudy and Chang, the Gibbs free energy of formation for $\text{CrC}_{3/7}$ at 1575°K was found to be $-9,940 \pm 1280$ cal/g-atom Cr. From this value and the available free energy functions for $\text{CrC}_{3/7}$, Cr, and C, the heat formation of $\text{CrC}_{3/7}$ at 298.15°K was found to be -8160 ± 1300 cal/g-atom.

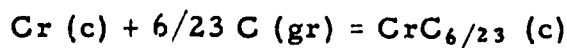
The Gibbs free energy of formation of $\text{CrC}_{3/7}$ as a function of temperature was calculated and the calculated data were fitted the following linear equation:



$$\Delta G_{f, 298.15 - 1600^\circ\text{K}} = - 7,910 + 1.27 \text{ T}$$



Again, based on the selected value of ΔG_f for $\text{CrC}_{2/3}$ and the values of ΔG_R for reactions (c) and (d) reported by Rudy and Chang, the Gibbs free energy of formation for $\text{CrC}_{6/23}$ at 1573°K was found to be $- 6,700 \pm 800$ cal/g-atom. From this value we derived a value of $\Delta H_{f, \text{st}} = - 5,670 \pm 850$ cal/g-atom Cr for $\text{CrC}_{6/23}$. The calculated Gibbs free energy of formation of $\text{CrC}_{6/23}$ based on the selected value of $\Delta H_{f, \text{st}}$ and the available free energy functions for $\text{CrC}_{6/23}$, Cr, and C, was fitted to the following equation:



$$\Delta G_{f, 298.15 - 1800^\circ\text{K}} = - 5,470 - 0.78 \text{ T}$$

b. Molybdenum - Carbon System

(1) Phase Diagram

The phase diagram of the molybdenum-carbon system, as shown in Figure 10, is taken from an earlier documentary report by Rudy, Windisch, and Chang⁽⁷⁷⁾. Among the four intermediate phases appearing in the molybdenum-carbon system, $\alpha\text{-Mo}_2\text{C}$

is the only phase stable at low temperatures. Both the $\alpha\text{-Mo}_2\text{C}$ and $\beta\text{-Mo}_2\text{C}$ phases have a hexagonal close-packed arrangement of the metal atoms, and the carbon sublattice of the $\alpha\text{-Mo}_2\text{C}$ phase was found to be ordered at room temperature using the neutron-diffraction method.⁽⁷⁸⁾ The η -phase has a hexagonal (pseudo cubic) lattice, while the $\alpha\text{-MoC}_{1-x}$ has a sodium chloride (B1) structure.

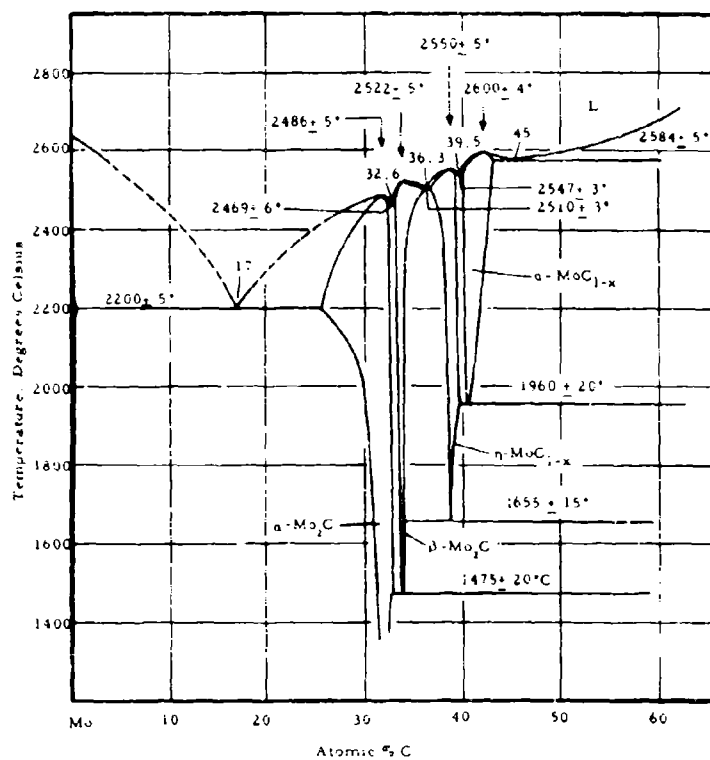


Figure 10. The Phase Diagram of Molybdenum-Carbon System

(2) Low-Temperature Data

There exist no experimental low-temperature heat capacity data for any of the molybdenum carbides. Krikorian⁽⁷⁹⁾ estimated a value of $S_{st} = 8.55 \pm 0.5$ cal/deg g-atom Mo for Mo_2C . Using the available entropy data for Mo⁽¹⁾ and graphite⁽⁴⁾, $\Delta S_{f, st} = 1.04 \pm 0.5$ cal/deg g-atom Mo was obtained.

(3) High-Temperature Data

No high-temperature heat content or heat capacity data were found in the literature for any of the carbides.

(4) Reaction Equilibrium Data

Gleiser and Chipman⁽⁸⁰⁾ studied the equilibrium $\text{Mo}-\alpha\text{-Mo}_{2.23}\text{C}-\text{MoO}_2\text{-CO-CO}_2$ over the temperature interval 1200 - 1340°K, and obtained $\Delta G_f = -11,710 - 1.83 T$ for the $\alpha\text{-Mo}_2\text{C}$ phase at the metal-rich phase boundary.

Schenck, Kurzen, and Wesselkock⁽⁸¹⁾ studied the equilibrium $\text{Mo}-\alpha\text{-Mo}_2\text{C}-\text{H}_2\text{-CH}_4$ at 973 and 1123°K. However, their results are doubtful since thermal segregation of the static gas mixture used must have occurred as originally pointed out by Richardson⁽⁴⁴⁾. Moreover, the thermodynamic data of CH_4 obtained by Schenck, et al. from a study of the equilibrium $\text{C-H}_2\text{-CH}_4$, using the same experimental method, do not agree with the presently accepted values.

Browning and Emmett⁽⁸²⁾ claimed to have studied the equilibrium $\text{Mo-Mo}_2\text{C-CH}_4\text{-H}_2$ over the temperature interval 820-952°K, and the equilibrium $\text{Mo}_2\text{C-CH}_4\text{-MoC-H}_2$ over the temperature interval 936-1098°K. According to Gleiser and Chipman⁽⁸⁰⁾, the first

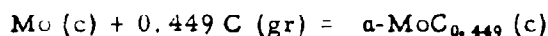
equilibrium yielded a rather large entropy change of about 26 e.u. for the reaction $2\text{Mo}(c) + \text{C}(\text{gr}) = \text{Mo}_2\text{C}(c)$. The second equilibrium studied is inconsistent with our presently established phase diagram since none of the other three intermediate phases, $\beta\text{-Mo}_2\text{C}$, $\eta\text{-MoC}_x$ and $\alpha\text{-MoC}_x$, is stable with respect to $\alpha\text{-Mo}_2\text{C}$ and graphite in this temperature range.

(5) Calorimetric Data

Mah⁽⁸²⁾ determined the heat of formation of Mo_2C calorimetrically and reported $\Delta H_{f, \text{st}} = -11,000 \pm 700 \text{ cal/2 g-atom Mo}$, which is in reasonable agreement with Gleiser and Chipman's result. The sample was prepared by direct combination of the elements at 1150°C under two atmospheres of H_2 . Chemical analysis of the sample showed 94.09% Mo and 5.89% C.

(6) Selection of Enthalpy and Free Energy Data

Based on the work of Gleiser and Chipman, the Gibbs free energy of formation equation selected for $\alpha\text{-MoC}_{0.447}$ is:



$$\Delta G_{f, 298.15 - 1340^\circ\text{K}} = -5250 - 0.82 T$$

The uncertainty in the ΔG_f value is estimated to be $\pm 700 \text{ cal/g-atom Mo}$.

c. Tungsten-Carbon System

(1) Phase Diagram

The phase diagram of the tungsten-carbon system, as shown in Figure 11, is based on the work of Rudy and

Windisch⁽⁸³⁾. Four intermediate phases appear in this system. The phases α - W_2C and β - W_2C are isostructural with α - Mo_2C and β - Mo_2C . The phase α - WC_x has a sodium chloride (B1) structure, while WC has a simple hexagonal structure. In contrast to the relative stabilities of the intermediate

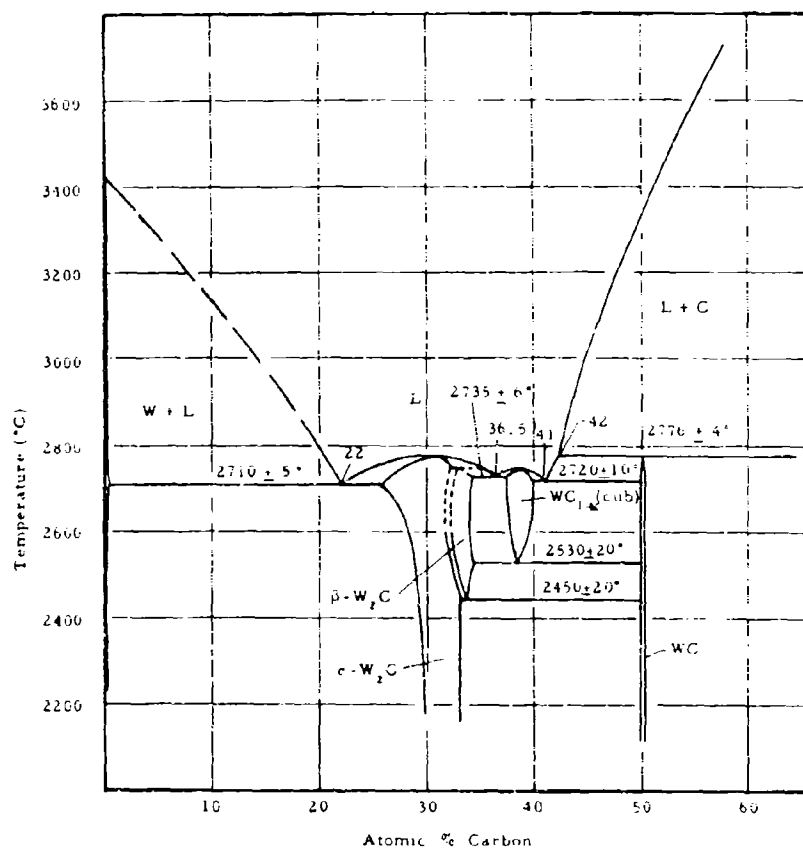


Figure 11. The Phase Diagram of the Tungsten-Carbon System

phases in the Mo-C system, the WC phase is the only stable phase at low temperatures.

(2) Low-Temperature Data

No low-temperature heat capacity data were found in the literature for any of the four intermediate phases.

(3) High-Temperature Data

Levinson⁽³³⁾ measured the heat content of $WC_{0.99}$ over the temperature interval 1276 - 2642°K. The sample had 93.97% W, 6.07% C, and less than 500 ppm free graphite; the apparent composition of the sample was $WC_{0.99}$. The calculated thermal properties of $WC_{0.99}$ based on the data of Levinson are reported in Table 9. The tabulated heat content of $WC_{0.99}$ over the temperature interval 1200 - 1700°K may be represented by the following analytical expression with an average standard deviation of 9 cal/g-atom W and a maximum deviation of 19 cal/g-atom W at 2700°K:

$$H_T - H_{st} = 10.417 T + 0.79755 \times 10^{-3} T^2 - 3562.8$$

(4) Reaction Equilibrium Data

Gleiser and Chipman⁽⁸⁴⁾ studied the equilibrium $WC-CO_2-W-CO$ over the temperature interval 1215 - 1266°K. At 1240°K, the average temperature of the equilibrium measurement, the Gibbs free energy of formation of WC which was derived is -8,340 cal/g-atom W.

Alekseev and Shvartsman⁽⁸⁵⁾ studied the equilibrium $W_2C-H_2-W-CH_4$ over the temperature interval 923 - 1173°K and the equilibrium $WC-H_2-W_2C-CH_4$ over the temperature interval 973 - 1273°K. From their measurements, Alekseev and Shvartsman derived $\Delta G_{f, WC} = -1,950 - 3.9 T$ and $\Delta G_{f, W_2C} = -7,550 + 1.16 T$. A

combination of the ΔG_f values for WC and W_2C does predict the correct temperature where W_2C decomposes into W and WC.

Orton⁽⁸⁶⁾ studied the equilibria:

$WC-H_2-W-CH_4$, $W_2C-H_2-W-CH_4$, and $WC-H_2-W_2C-CH_4$ over the temperature interval 1173 - 1773°K. From his equilibrium measurements, Orton derived $\Delta G_{f, WC} = -1,947 + 0.40 T$ and $\Delta G_{f, W_2C} = +46,420 - 32.12 T$. The ΔG_f values obtained by Orton appears to be in error when compared with the direct calorimetric values obtained by Mah.

(5) Vapor Pressure Data

Coffman, Kibler, Lyon, and Acchione⁽¹³⁾

studied the Langmuir vaporization of WC over the temperature interval 2319 - 2667°K. After initial vaporization, they found W_2C on the surface of the WC sample, in agreement with the established phase diagram. Hoch, Blackburn, Dingley, and Johnston⁽⁶⁴⁾ measured the vapor pressure of carbon over WC over the temperature interval 2170 - 2770°K, and found that the vapor pressure was essentially the same as the vapor pressure of pure graphite.

(6) Calorimetric Data

McGraw, Seltz, and Snyder⁽⁸⁷⁾

determined the heat of combustion of WC to be $-285,800 \pm 700$ cal/g-mole WC. Recently Mah⁽⁸²⁾ redetermined the heat of combustion of WC to WO_3 and CO_2 to be $-285,940$ cal/g-mole WC, in perfect agreement with McGraw's value. Based on the average value of the two combustion results and the available heats of formation for WO_3 and CO_2 ⁽⁴⁾, the heat of formation of WC was found to be $-9,670 \pm 400$ cal/g-atom W. Chemical analysis of the WC sample showed it to contain 93.90% W and 6.10% C. For the purpose of

Table 9. High-Temperature Thermal Properties of WC_{0.99}

| T, °K | C _p | H _T -H _{st} | ΔC _p |
|-------|----------------|---------------------------------|-----------------|
| 1200 | 12.19 | 10,100 | 0.14 |
| 1300 | 12.39 | 11,330 | 0.17 |
| 1400 | 12.58 | 12,583 | 0.20 |
| 1500 | 12.77 | 13,845 | 0.25 |
| 1600 | 12.96 | 15,141 | 0.30 |
| 1700 | 13.14 | 16,444 | 0.35 |
| 1800 | 13.31 | 17,767 | 0.41 |
| 1900 | 13.48 | 19,110 | 0.46 |
| 2000 | 13.64 | 20,456 | 0.50 |
| 2100 | 13.79 | 21,838 | 0.55 |
| 2200 | 13.92 | 23,222 | 0.58 |
| 2300 | 14.07 | 24,623 | 0.61 |
| 2400 | 14.20 | 26,042 | 0.64 |
| 2500 | 14.34 | 27,479 | 0.69 |
| 2600 | 14.47 | 28,911 | 0.72 |
| 2700 | 14.60 | 30,359 | 0.74 |

correcting the calorimetric value, the composition was considered to be 99.47% WC and 0.53% W since W lines were detected by X-ray diffraction technique.

Mah⁽⁸²⁾ also determined the heat of formation of α-WC_{1/2} to be - 3,150 ± 300 cal/g-atom W. The chemical composition of this sample was considered to be 95.08% W₂C, 2.92% W, and 2.0% WC, and the calorimetric results were corrected accordingly.

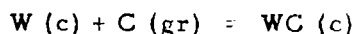
(7) Selection of Enthalpy and Free Energy Data

(a) WC-Phase

The selected value of the heat of formation of $WC_{1.0}$ at 298.15°K is $-9,670 \pm 400$ cal/g-atom W, based on the data of McGraw, et.al., and of Mah. Using the available heat content data for WC, $W^{(1)}$, and $C^{(4)}$;

$$\Delta H_{f, 1240^\circ K} = -9,090 \pm 500 \text{ cal/g-atom W}$$

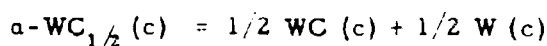
was obtained for $WC_{1.0}$. Based on the ΔG_f value of Gleiser and Chipman for WC, $\Delta S_{f, 1240^\circ K} = 0.60 \pm 0.5$ cal/deg g-atom W. Using the available values of $S_{1240^\circ K}$ for $W^{(1)}$ and $C^{(4)}$, a value of $S_{WC, 1240^\circ K} = 23.20$ cal/deg g-atom was obtained. Based on the selected values of ΔH_f and ΔG_f for WC at 1240°K and the available thermal data, the Gibbs free energy of formation of WC from 1200 to 2700°K was calculated, and the calculated values were fitted to the following linear equation:



$$\Delta G_{f, 1200-2700^\circ K} = -8,905 + 0.47 T$$

(b) α - $WC_{1/2}$

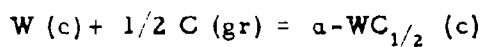
The selected value of the heat of formation of $WC_{1/2}$ at 298.15°K is $-3,150 \pm 300$ cal/g-atom W, based on the data of Mah. Since α - WC_2 decomposes to WC and W at 1523°K, the Gibbs free energy change at this temperature is zero for the reaction:



For lack of data, we have assumed that ΔC_p to be zero for $\alpha\text{-WC}_{1/2}$, even though we expect that this would not be true. With this assumption, and using the selected value of ΔG_f for WC, we obtain

$$\Delta S_{f, \alpha\text{-WC}_{1/2}} = 0.62 \pm 0.5 \text{ cal/deg g-atom W}$$

at 1523°K. The selected Gibbs free energy of formation equation for $\alpha\text{-WC}_{1/2}$ is:



$$\Delta G_f = -3,150 - 0.62T$$

III. CALCULATION OF THERMODYNAMIC PROPERTIES OF NON-STOICHIOMETRIC BINARY CARBIDES

In order to calculate the phase diagrams of the ternary and higher-order systems, the Gibbs free energy-composition-temperature diagrams of the binary phases must be available. Unfortunately, as the evaluation of the thermodynamic properties of the binary carbides revealed, the compositional variation of the Gibbs free energy is not available for any of the binary carbide phases. To overcome this deficiency, we shall calculate the Gibbs free energies of the alloy phases as a function of composition based on theoretical models.

In the following section, we shall first discuss the interstitial model as applied to the terminal solid solutions such as the $\alpha\text{-Hf}$ solid solution, and the vacancy model of Schottky and Wagner as applied to all the mono-carbide phases (B1).

Based on the theoretical models, the selected thermodynamic properties of alloy phases at the stoichiometric composition, and the

available phase diagrams, the Gibbs free energy of formation of the alloy phases as a function of composition will be calculated and the results reported.

In this section, we shall express all the thermodynamic quantities in terms of one gram atom of alloy instead of one gram atom of metal as done in the previous section. Again, we shall use the elements in the stable form at the temperature and one atmosphere pressure as the standard state.

A. THEORETICAL MODEL

1. Interstitial Model as Applied to the Terminal Solid Solution

The Gibbs free energy of formation of a binary interstitial carbon solid solution, $\text{Me}_{1-x}\text{C}_x$ (where Me stands for the transition metal, C stands for carbon and x is the atom fraction of carbon in the solution), from the component elements arises from two contributions which are thermal and configurational. Since the experimental heat and entropy data of the $\text{Me}_{1-x}\text{C}_x$ are not available as a function of composition, we shall assume that the thermal free energy of formation of $\text{Me}_{1-x}\text{C}_x$ is proportional to the concentration of carbon. The configurational free energy of formation is entirely due to the entropy of mixing of the interstitial carbon atoms among the available sites.

According to Boltzmann, the entropy of mixing is related to the thermodynamic probability by the following formula:

$$S_{\text{mix}} = k \ln W \quad (1)$$

where S_{mix} stands for the entropy of mixing, k is the Boltzmann constant, and W is the thermodynamic probability.

We shall now evaluate the thermodynamic probability,

W , in the following manner based on one gram atom alloy. Let

- N = Total number of atoms in an alloy, i.e. number of metal atoms plus number of carbon atoms
- xN = Number of carbon atoms on the interstitial sites
- $(1-x)N$ = Number of metal (or host) atoms
- N_i = Number of interstitial sites
- $N_i - xN$ = Number of unoccupied interstitial sites

The thermodynamic probability is

$$W = \frac{N_i!}{(xN)! (N_i - xN)!} \quad (2)$$

Using Stirling's approximation for the factorial terms in equation (2), the entropy of mixing is reduced to

$$S_{\text{mix}} = -k N_i \ln \left(\frac{N_i - xN}{N_i} \right) + xN k \ln \left(\frac{N_i - xN}{xN} \right) \quad (3)$$

Since there is one octahedral interstitial hole per host atom in a hexagonal close-packed structure, such as $\alpha\text{-Hf}$, the number of interstitial holes is

$$N_i = (1-x)N \quad (4)$$

After substituting N_i into equation (3), we have

$$S_{\text{mix}} = -R (1-x) \ln \left(\frac{1-2x}{1-x} \right) + xR \ln \left(\frac{1-2x}{x} \right) \quad (5)$$

where $R = kN$ is the universal gas constant.

From equation (5) and the assumption we made earlier with regard to the thermal contribution to the free energy of $\text{Me}_{1-x}\text{C}_x$, we have

$$\Delta G_f = Bx + RT \left[x \ln \left(\frac{x}{1-2x} \right) + (1-x) \ln \left(\frac{1-2x}{1-x} \right) \right] \quad (6)$$

In this expression, Bx is the thermal contribution and B is constant which will be evaluated for $\alpha\text{-Hf}$ terminal solid solution in the next section.

Since the addition of interstitial carbon atoms to the host lattice is limited by the available number of interstitial sites, the value of x in equation (6) can never exceed 0.5. In practice, the value of x does not even approach 0.5, because the occupation of one interstitial site causes the neighboring site to become energetically unfavorable. However, for our purpose here, we shall not refine equation (6) by introducing new parameters since we do not have a sufficient number of boundary conditions to evaluate all the parameters.

From equation (6) and the well-known thermodynamic equations relating the partial molar and integral free energies,

$$\Delta \bar{G}_{\text{Me}} = \Delta G - x \frac{\partial \Delta G}{\partial x} \quad (7)$$

$$\Delta \bar{G}_{\text{C}} = \Delta G + (1-x) \frac{\partial \Delta G}{\partial x} \quad (8)$$

we obtain the following equations for the partial molar free energies of the metal and carbon components in the terminal α -solid solution:

$$\Delta \bar{G}_{\text{Me}} = RT \ln \left(\frac{1-2x}{1-x} \right) \quad (9)$$

$$\Delta \bar{G}_{\text{C}} = B + RT \ln \left(\frac{x}{1-2x} \right) \quad (10)$$

2. Schottky-Wagner Vacancy Model

The thermodynamic model of non-stoichiometric alloy phases originally formulated by Schottky and Wagner⁽⁸⁹⁾ was discussed in detail by Wagner⁽⁹⁰⁾ and more recently by Kaufman, Bernstein and Sarney⁽⁹¹⁾ who applied this model to the monocarbide phases. The model alloys contain two sublattices in the crystal. In the case of the binary carbide phases, the two sublattices are respectively the metal and carbon sublattices. Due to the large size difference of the metal and carbon atoms, contributions from exchanges of atoms among the two sublattices can be neglected. Assuming the only defects present in the lattice are carbon vacancies and metal vacancies, the Gibbs free energy of formation of an alloy phase, $\text{Me}_{1-x}\text{C}_x$, from the component elements arises from the following contributions:

- a. The formation of an ordered alloy at the stoichiometric composition,
- b. The creation of carbon vacancies,
- c. The creation of metal vacancies,
- d. The free energy of mixing between the metal atoms and vacancies on the metal sublattice, and between the carbon atoms and vacancies on the carbon sublattice.

Mathematically, the Gibbs free energy of formation of an alloy, $\text{Me}_{1-x}\text{C}_x$, in terms of one gram atom alloy may be expressed as follows:**

**The derivation of the Schottky-Wagner equations follows closely that of Kaufman, et.al.⁽⁹¹⁾

$$\Delta G_{f,x} = \frac{N_s}{N} \Delta G_{f,x_0}^* + \frac{N_{Me^+}}{N} G_{Me^+} + \frac{N_{C^+}}{N} G_{C^+} - TS_{mix} \quad (11)$$

In this equation, $\Delta G_{f,x_0}^*$ is the free energy of formation of an ordered alloy at the stoichiometric composition, $Me_{1-x_0}C_{x_0}$; G_{Me^+} and G_{C^+} are the free energies of creating a metal vacancy on the metal sublattice and of creating a carbon vacancy on the carbon sublattice, respectively; N_s , N_{Me^+} , and N_{C^+} are the total number of lattice sites, the total number of atoms, the number of vacant metal sites, and the number of vacant carbon sites; x is the atom fraction of carbon; and x_0 is the stoichiometric composition. The entropy of mixing, S_{mix} , in equation (11) arises from the mixing between the metal atoms and vacant sites on the metal sublattice; and from the mixing between the carbon atoms and vacant sites on the carbon sublattice.

The entropy of mixing, derived in the usual manner as done in the previous section, is:

$$S_{mix} = - \left[(1-x_0) N_s - N_{Me^+} \right] \ln \left[\frac{(1-x_0) N_s - N_{Me^+}}{(1-x_0) N_s} \right] - N_{Me^+} \ln \left[\frac{N_{Me^+}}{(1-x_0) N_s} \right] \\ - (x_0 N_s - N_{C^+}) \ln \left(\frac{x_0 N_s - N_{C^+}}{x_0 N_s} \right) - N_{C^+} \ln \left(\frac{N_{C^+}}{x_0 N_s} \right) \quad (12)$$

Introducing the new variables: $n_{Me^+} = \frac{N_{Me^+}}{N}$, $n_{C^+} = \frac{N_{C^+}}{N}$, and $y = \frac{N_s}{N}$; the Gibbs free energy of formation of an alloy, $Me_{1-x}C_x$, becomes:

$$\Delta G_{f,x} = y \Delta G_{f,x_0}^* + n_{Me^+} G_{Me^+} + n_{C^+} G_{C^+} + RT \left\{ n_{Me^+} \ln \left[\frac{n_{Me^+}}{(1-x_0)y} \right] \right. \\ \left. + n_{C^+} \ln \left(\frac{n_{C^+}}{x_0 y} \right) + \left[(1-x_0)y - n_{Me^+} \right] \ln \left[\frac{(1-x_0)y - n_{Me^+}}{(1-x_0)y} \right] \right. \\ \left. + \left[x_0 y - n_{C^+} \right] \ln \left(\frac{x_0 y - n_{C^+}}{x_0 y} \right) \right\} \quad (13)$$

With a fixed composition at constant pressure and temperature, the Gibbs free energy, as written in (13), is minimized according to the method of Lagrange with the two following constraints arising from the conservation of masses:

$$\phi_1 = (1-x) - (1-x_0)y + n_{Me^+} = 0 \quad (14a)$$

$$\phi_2 = x - x_0y + n_{C^+} = 0 \quad (14b)$$

Accordingly, we have:

$$\frac{\partial \Delta G_f}{\partial n_{Me^+}} + \lambda_1 \frac{\partial \phi_1}{\partial n_{Me^+}} + \lambda_2 \frac{\partial \phi_2}{\partial n_{Me^+}} = 0 \quad (15a)$$

$$\frac{\partial \Delta G_f}{\partial n_{C^+}} + \lambda_1 \frac{\partial \phi_1}{\partial n_{C^+}} + \lambda_2 \frac{\partial \phi_2}{\partial n_{C^+}} = 0 \quad (15b)$$

$$\frac{\partial \Delta G_f}{\partial y} + \lambda_1 \frac{\partial \phi_1}{\partial y} + \lambda_2 \frac{\partial \phi_2}{\partial y} = 0 \quad (15c)$$

In these equations λ_1 and λ_2 are the undetermined multipliers. Performing the differentiation of ϕ_1 and ϕ_2 , and substituting the results into equations (15), we have from equations (15a) and (15b):

$$\lambda_1 = - \frac{\partial \Delta G_f}{\partial n_{Me^+}}$$

$$\lambda_2 = - \frac{\partial \Delta G_f}{\partial n_{C^+}}$$

From equation (15c) we obtain:

$$\frac{\partial \Delta G_f}{\partial y} + (x_0 - 1) \lambda_1 - x_0 \lambda_2 = 0$$

Thus, the conditional equation, when $\Delta G_{f,x}$ is a minimum, is:

$$\frac{\partial \Delta G_f}{\partial y} + (1-x_o) \frac{\partial \Delta G_f}{\partial n_{Me^+}} + x_o \frac{\partial \Delta G_f}{\partial n_{C^+}} = 0 \quad (16)$$

We now proceed to differentiate ΔG_f with respect to y , n_{Me^+} , and n_{C^+} ; and we obtain:

$$\frac{\partial \Delta G_f}{\partial n_{Me^+}} = G_{Me^+} + RT \left\{ \ln \left[\frac{n_{Me^+}}{(1-x_o)y} \right] - \ln \left[\frac{(1-x_o)y - n_{Me^+}}{(1-x_o)y} \right] \right\} \quad (17a)$$

$$\frac{\partial \Delta G_f}{\partial n_{C^+}} = G_{C^+} + RT \left\{ \ln \left(\frac{n_{C^+}}{x_o y} \right) - \ln \left(\frac{x_o y - n_{C^+}}{x_o y} \right) \right\} \quad (17b)$$

$$\frac{\partial \Delta G_f}{\partial y} = \Delta G_{f,x_o}^* + RT \left\{ (1-x_o) \ln \left[\frac{(1-x_o)y - n_{Me^+}}{(1-x_o)y} \right] + x_o \ln \left(\frac{x_o y - n_{C^+}}{x_o y} \right) \right\} \quad (17c)$$

After the substitution of $\frac{\partial \Delta G_f}{\partial n_{Me^+}}$, $\frac{\partial \Delta G_f}{\partial n_{C^+}}$, and $\frac{\partial \Delta G_f}{\partial y}$; and rearrangement of terms, equation (16) becomes:

$$\begin{aligned} \Delta G_{f,x_o}^* - (1-x_o) \left[-G_{Me^+} + RT \ln (1-x_o) \right] - x_o \left[-G_{C^+} + RT \ln x_o \right] \\ = - (1-x_o) RT \ln \left(\frac{n_{Me^+}}{y} \right) - x_o RT \ln \left(\frac{n_{C^+}}{y} \right) \end{aligned} \quad (18)$$

From equations (14a) and (14b), we have:

$$n_{Me^+} = y (1-x_o) - (1-x)$$

$$n_{C^+} = x_o y - x$$

Substitution of n_{Me^+} and n_{C^+} into (18) yields:

$$\begin{aligned}\Delta G_{f, x_0}^* &= (1-x_0) \left[-G_{\text{Me}^+} + RT \ln (1-x_0) \right] - x_0 \left(-G_{\text{C}^+} + RT \ln x_0 \right) \\ &= -RT \left\{ (1-x_0) \ln \left[\frac{y(1-x_0) - (1-x)}{y} \right] + x_0 \ln \left(\frac{x_0 y - x}{y} \right) \right\}\end{aligned}$$

Let us now introduce a new parameter, a , which is defined by the equation:

$$\ln a = (1-x_0) \ln \left[\frac{y(1-x_0) - (1-x)}{y} \right] + x_0 \ln \left(\frac{x_0 y - x}{y} \right) \quad (19)$$

We then have the following conditional equation for the minimization of the free energy of an alloy $\text{Me}_{1-x}\text{C}_x$:

$$\begin{aligned}-RT \ln a &= \Delta G_{f, x_0}^* - (1-x_0) \left[-G_{\text{Me}^+} + RT \ln (1-x_0) \right] \\ &\quad - x_0 \left[-G_{\text{C}^+} + RT \ln x_0 \right]\end{aligned} \quad (20)$$

We shall now derive $\Delta G_{f, x}$ as a function of x by substituting n_{Me^+} and n_{C^+} into equation (13) and the partial molar quantities, $\Delta \bar{G}_{\text{Me}}$ and $\Delta \bar{G}_{\text{C}}$, using equations (7) and (8). The resulting equations are:

$$\begin{aligned}\Delta G_{f, x} &= y \Delta G_{f, x_0}^* + \left[y(1-x_0) - (1-x) \right] G_{\text{Me}^+} + \left[x_0 y - x \right] G_{\text{C}^+} \\ &+ RT \left\{ \left[y(1-x_0) - (1-x) \right] \ln \left[\frac{y(1-x_0) - (1-x)}{(1-x_0)y} \right] + (x_0 y - x) \ln \left(\frac{x_0 y - x}{x_0 y} \right) \right. \\ &\quad \left. + (1-x) \ln \left[\frac{1-x}{(1-x_0)y} \right] + x \ln \left(\frac{x}{x_0 y} \right) \right\}\end{aligned} \quad (21a)$$

$$\Delta \overline{G}_{Me} = -G_{Me^+} + RT \ln \left[\frac{1-x}{(1-x_0)y - (1-x)} \right] \quad (21b)$$

$$\Delta \overline{G}_C = -G_{C^+} + RT \ln \left(\frac{x}{x_0 y - x} \right) \quad (21c)$$

From equations (19) and (21), the integral free energy of formation and the partial molar free energies of the metal and the carbon component in the alloy at the stoichiometric composition, $Me_{1-x_0}C_{x_0}$ become:

$$\Delta G_{f, x_0} = \Delta G_{f, x_0}^* + RT \ln \left[1 - \frac{a}{(1-x_0)^{(1-x_0)} x_0 x_0} \right] \quad (22a)$$

$$\Delta \overline{G}_{Me, x_0} = -G_{Me^+} + RT \ln \left[\frac{x_0^{x_0} (1-x_0)^{(1-x_0)}}{a} - 1 \right] \quad (22b)$$

$$\Delta \overline{G}_{C, x_0} = -G_{C^+} + RT \ln \left[\frac{x_0^{x_0} (1-x_0)^{(1-x_0)}}{a} - 1 \right] \quad (22c)$$

$$a = x_0^{x_0} (1-x_0)^{(1-x_0)} \frac{y-1}{y} = x_0^{x_0} (1-x_0)^{(1-x_0)} \left(\frac{N_s - N}{N_s} \right) \quad (22d)$$

Application of these equations for values of x smaller or greater than x_0 are complicated by the fact that y is a complicated function of a . However, for small values of a , i.e. when a is smaller than 1%, these equations may be simplified. Let us rearrange equation (19) as follows:

$$(ay)^{\frac{1}{x_0}} = [x_0 y - x] \left[y(1-x_0) - (1-x) \right] - \left(1 - \frac{1}{x_0} \right)$$

One can see from the above equation, that when a is small, $y \approx \frac{1-x}{1-x_0}$ for values of x smaller than x_0 , and $y \approx \frac{x}{x_0}$ for values of x greater than x_0 .

Thus, we have for $x < x_0$:

$$\Delta \bar{G}_{Me} = -G_{Me^+} + \frac{RT}{1-x_0} \ln \frac{(1-x_0)^{(1-x_0)} (x_0-x)^{x_0}}{(1-x_0)^{x_0} a} \quad (23a)$$

$$\Delta \bar{G}_C = -G_{C^+} + RT \ln \frac{x(1-x_0)}{(x_0-x)} \quad (23b)$$

and for $x > x_0$:

$$\Delta \bar{G}_{Me} = -G_{Me^+} + RT \ln \left[\frac{x_0(1-x)}{(x-x_0)} \right] \quad (24a)$$

$$\Delta \bar{G}_C = -G_{C^+} + \frac{RT}{x_0} \ln \left[\frac{x^{(x_0-1)} x_0^{x_0} (x-x_0)^{(1-x_0)}}{a} \right] \quad (24b)$$

For the monocarbide phases, $Me_{1-x_0}C_{x_0}$, where $x_0 = 0.5$, equation (21) is greatly simplified and we have:

$$\begin{aligned} \Delta G_{f,x} = & [0.5 y - (1-x)] G_{Me^+} + [0.5 y - x] G_{C^+} + y \Delta G_{f,as}^* \\ & + RT \left\{ [0.5 y - (1-x)] \ln \left[\frac{0.5 y - (1-x)}{0.5 y} \right] + (0.5 y - x) \ln \left(\frac{0.5 y - x}{0.5 y} \right) \right. \\ & \left. + (1-x) \ln \left(\frac{1-x}{0.5 y} \right) + x \ln \left(\frac{x}{0.5 y} \right) \right\} \end{aligned} \quad (25a)$$

$$\Delta \bar{G}_{Me} = -G_{Me^+} + RT \ln \left[\frac{1-x}{0.5 y - (1-x)} \right] \quad (25b)$$

$$\Delta \bar{G}_C = -G_{C^+} + RT \ln \left(\frac{x}{0.5 y - x} \right) \quad (25c)$$

The conditional equation when the total free energy is a minimum is:

$$-2RT \ln a = 2\Delta G_{f,0.5}^* + G_{Me^+} + G_{C^+} + 2RT \ln 2 \quad (26)$$

$$\ln a = 0.5 \ln \left[\frac{0.5 y - (1-x)}{y} \right] + 0.5 \ln \left(\frac{0.5 y - x}{y} \right) \quad (27a)$$

$$y = \frac{1 + [1-4x(1-x)(1-4a)]^{1/2}}{(1-4a^2)} \quad (27b)$$

At the stoichiometric composition, $x_0 = 0.5$, equation (22) yields:

$$\Delta G_{f,0.5} = \Delta G_{f,0.5}^* + RT \ln (1-2a) \quad (28a)$$

$$\Delta \bar{G}_{Me,0.5} = -G_{Me^+} + RT \ln \left(\frac{1-2a}{a} \right) \quad (28b)$$

$$\Delta \bar{G}_{Me,0.5} = -G_{C^+} + RT \ln \left(\frac{1-2a}{a} \right) \quad (28c)$$

Equation (22d) reduces to:

$$a = 0.5 \left(\frac{y-1}{y} \right) = 0.5 \left(\frac{N_s - N}{N_s} \right) = \frac{N_{Me^+}}{N_s} = \frac{N_{C^+}}{N_s} \quad (29)$$

We see from (29) that a is equal to the fraction of the vacant metal sites or vacant carbon sites at $x_0 = 0.5$. However, this is no longer true for values of x deviating from the stoichiometric composition, $x_0 = 0.5$.

For values of x deviating from x_0 , for example when $x < 0.5$, and for small values of a , i.e. less than 1%, we have the following approximate expressions for the partial molar free energies of the metal and carbon component in the carbide phase:

$$\Delta \overline{G}_{Me} = -G_{Me^+} + RT \ln \left[\frac{1-2x}{4(1-x)a^2} \right] \quad (30a)$$

$$\Delta \overline{G}_C = -G_{C^+} + RT \ln \left(\frac{x}{1-2x} \right) \quad (30b)$$

For the case when $x > 0.5$ we have:

$$\Delta \overline{G}_{Me} = -G_{Me^+} + RT \ln \left(\frac{1-x}{2x-1} \right) \quad (31a)$$

$$\Delta \overline{G}_C = -G_{C^+} + RT \ln \left(\frac{2x-1}{4xa^2} \right) \quad (31b)$$

According to equation (28a), when a is small, $RT \ln (1-a)$ approaches zero, and we have:

$$\Delta G_{f, 0.5} = \Delta G_{f, 0.5}^*$$

With this condition and when $x < 0.5$, equations (26), (30), and (31) yield the results:

$$\Delta \overline{G}_{Me} = G_{C^+} + 2\Delta G_{f, 0.5} + RT \ln \left(\frac{1-x}{1-x} \right) \quad (32a)$$

$$\Delta \overline{G}_C = -G_{C^+} + RT \ln \left(\frac{x}{1-2x} \right) \quad (32b)$$

For the case when $x > 0.5$, we have:

$$\Delta \overline{G}_{Me} = -G_{Me^+} + RT \ln \left(\frac{1-x}{2x-1} \right) \quad (33a)$$

$$\Delta \overline{G}_C = G_{Me^+} + 2\Delta G_{f, 0.5} + RT \ln \left(\frac{2x-1}{x} \right) \quad (33b)$$

B. CALCULATED THERMODYNAMIC PROPERTIES OF BINARY CARBIDES

1. Hafnium-Carbon System

The theoretical models presented in the previous sections will be now applied to the hafnium-carbon system. As shown in Figure 3, the addition of carbon atoms to α -Hf (hcp) stabilizes this structure to high temperatures at which pure α -Hf is unstable with respect to β -Hf (bcc). Moreover, the solubility of carbon in α -Hf at high temperature is rather large. In order to calculate the compositional variation of the Gibbs free energy of α -Hf terminal solid solution and of the monocarbide phase (designated by γ) at different temperatures, we must evaluate the four parameters: B , G_{Hf^+} , G_{C^+} , and a .

Kaufman, et.al.⁽⁹¹⁾ determined the three parameters of the Schottky-Wagner model for the monocarbides by using two pieces of experimental data, i.e. $\Delta\bar{G}_{\text{C}, x=0.5}^{\gamma} \approx 0$ and $\Delta\bar{G}_{\text{Me}, x=0.5}^{\gamma} \approx 2\Delta G_{f, 0.5}$, and an assumption relating the third parameter, a , to the heat of formation at absolute zero. However, we shall evaluate the three parameters: G_{Hf^+} , G_{C^+} , and a for HfC phase, and the parameter B , for α -Hf terminal solid solution, by the following four experimental conditions:

$$\text{a.} \quad \Delta\bar{G}_{\text{C}, x=0.5}^{\gamma} = 0 \quad (34\text{a})$$

$$\text{b.} \quad \Delta\bar{G}_{\text{Hf}, x=0.5}^{\gamma} = 2\Delta G_{f, 0.5} \quad (34\text{b})$$

$$\text{c.} \quad \Delta\bar{G}_{\text{Hf}, x_{\alpha\gamma}}^a = \Delta\bar{G}_{\text{Hf}, x_{\gamma a}}^{\gamma} \quad (34\text{c})$$

$$\text{d.} \quad \Delta\bar{G}_{\text{C}, x_{\alpha\gamma}}^a = \Delta\bar{G}_{\text{C}, x_{\gamma a}}^{\gamma} \quad (34\text{d})$$

In these equations $\Delta G_{f,0,s}$ is the Gibbs free energy of formation of HfC, expressed in terms of one gram atom alloy; and $x_{\alpha\gamma}$ and $x_{\gamma\alpha}$ are the phase boundaries of the α -phase and the γ -phase in the $\alpha+\gamma$ two-phase fields.

When a is small, as shown later to be the case for the HfC phase, from equations (28) and (32), we have:

$$G_{C+} = -RT \ln 2a \quad (35a)$$

$$G_{Hf+} = G_{C+} - 2\Delta G_{f,0,s} \quad (35b)$$

$$\Delta \bar{G}_{Hf, x_{\gamma\alpha}}^{\gamma} = G_{C+} + 2\Delta G_{f,0,s} + RT \ln \left(\frac{1-2x_{\gamma\alpha}}{1-x_{\gamma\alpha}} \right) \quad (36a)$$

$$\Delta \bar{G}_{C, x_{\gamma\alpha}}^{\gamma} = -G_{C+} + RT \ln \left(\frac{x_{\gamma\alpha}}{1-2x_{\gamma\alpha}} \right) \quad (36b)$$

The integral and partial molar free energies for the α -phase are given by equations (6), (9), and (10). However, at temperatures higher than the α - β transformation temperature of Hf, we must modify equations (6), (9), and (10) to include the free energy of transformation of α -Hf to β -Hf, since β -hafnium at the temperatures of interest has a different crystal structure from the α -terminal solid solution. The free energy of transformation of Hf may be approximated to be:

$$\Delta G_{Hf}^{\alpha \rightarrow \beta} = 0.9(2073-T) \quad (37)$$

The assumption we made in equation (37) is that $C_{p,\beta} - C_{p\alpha} = 0$, a condition which is true to a first approximation. Accordingly, at temperatures higher than $T_{\alpha-\beta}$, we have:

$$\Delta \bar{G}_{\text{Hf}, x_{a\gamma}}^a = -\Delta G_{\text{Hf}}^{a-\beta} + RT \ln \left(\frac{1-2x_{a\gamma}}{1-x_{a\gamma}} \right) \quad (38a)$$

$$\Delta \bar{G}_{\text{C}, x_{a\gamma}}^a = -\Delta G_{\text{Hf}}^{a-\beta} + B + RT \ln \left(\frac{x_{a\gamma}}{1-2x_{a\gamma}} \right) \quad (38b)$$

From equations (34) and (38), from the phase boundaries as shown in Figure 3, and from the selected values of $\Delta G_{f, 0.5}$, the values of G_{Hf} , G_{C} , a , and B were obtained. We found that both G_{Hf} and G_{C} decrease linearly with temperature, but a increases with temperature and B may be approximated by a constant, - 39,150 cal/g-atom.

The integral Gibbs free energies of formation of α -Hf terminal solid solution and the partial molar quantities now become:

$$\Delta G_{f, x}^a = -0.9 (2073-T) - 39,150 x + RT \left[x \ln \left(\frac{x}{1-2x} \right) + (1-x) \ln \left(\frac{1-2x}{1-x} \right) \right] \quad (39a)$$

$$\Delta \bar{G}_{\text{Hf}}^a = -0.9 (2073-T) + RT \ln \left(\frac{1-2x}{1-x} \right) \quad (39b)$$

$$\Delta \bar{G}_{\text{C}}^a = -0.9 (2073-T) - 39,150 x + RT \ln \left(\frac{x}{1-2x} \right) \quad (39c)$$

At temperatures below $T_{\alpha-\beta}$, the first term on the right hand side of the above equations drops out, but at temperatures higher than $T_{\beta-L}$, we must also include the free energies of melting of hafnium, $\Delta G_{\text{Hf}}^{\beta \rightarrow L}$.

Since the numerical calculation of ΔG , $\Delta \bar{G}_{\text{Hf}}$ and $\Delta \bar{G}_{\text{C}}$ for the monocarbide phase (γ -phase) is time-consuming, a computer program has been prepared to calculate the integral and partial molar

free energies as a function of temperature and composition according to equations (28), (32), and (33, based on the following conditions:

$$a. \quad G_{C+} = 55,860 - 2.1 T \quad (40)$$

$$b. \quad \Delta \bar{G}_{C, x \approx 0.5} \approx 0, \text{ which yields } G_{C+} = RT \ln 2a \quad (35a)$$

$$c. \quad \Delta \bar{G}_{Hf, x \approx 0.5} \approx 2\Delta G_{f, 0.5} \text{ which yields}$$

$$G_{Hf+} = G_{C+} - 2\Delta G_{f, 0.5} \quad (35b)$$

At 2273°K, $G_{Hf+} = 99,960$, $G_{C+} = 51,720$, and $a = 0.9345 \times 10^{-6}$. The values of ΔG , $\Delta \bar{G}_{Hf}$, and $\Delta \bar{G}_C$ as a function of composition for the α -phase, β -phase, and γ -phase in the hafnium-carbon system are shown in Figures 12a, 12b, and 13.

2. Zirconium-Carbon and Titanium-Carbon Systems

In contrast to the behavior of hafnium-carbon system, the addition of carbon atoms to the hcp form of zirconium and titanium does not stabilize the hcp terminal solid solution to temperatures higher than $T_{\alpha-\beta}$ of the pure metal. This simplifies the thermodynamic analysis since the metal component in the monocarbide phase (γ -phase) at the metal phase boundary is in equilibrium with the bcc form of the pure metal at temperatures higher than $T_{\alpha-\beta}$.

Using the boundary conditions similar to those expressed by equations (34a), (34b), and (34c); and based on the existing phase diagrams and the selected Gibbs free energies of formation of the monocarbide phases at the stoichiometric composition, the three

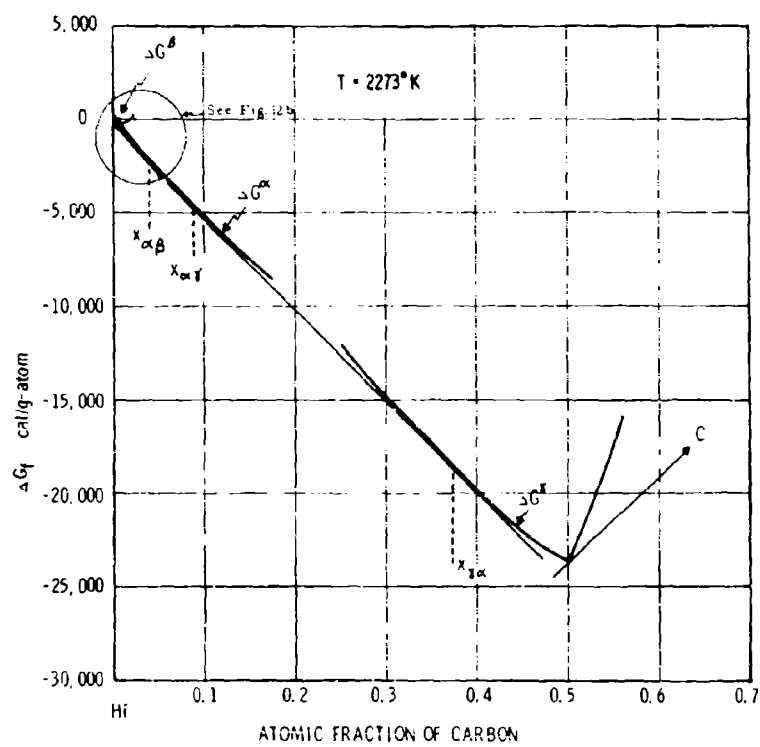


Figure 12a. Gibbs Free Energies of Formation of the α -, β -, and γ -phases in the Hafnium-Carbon System

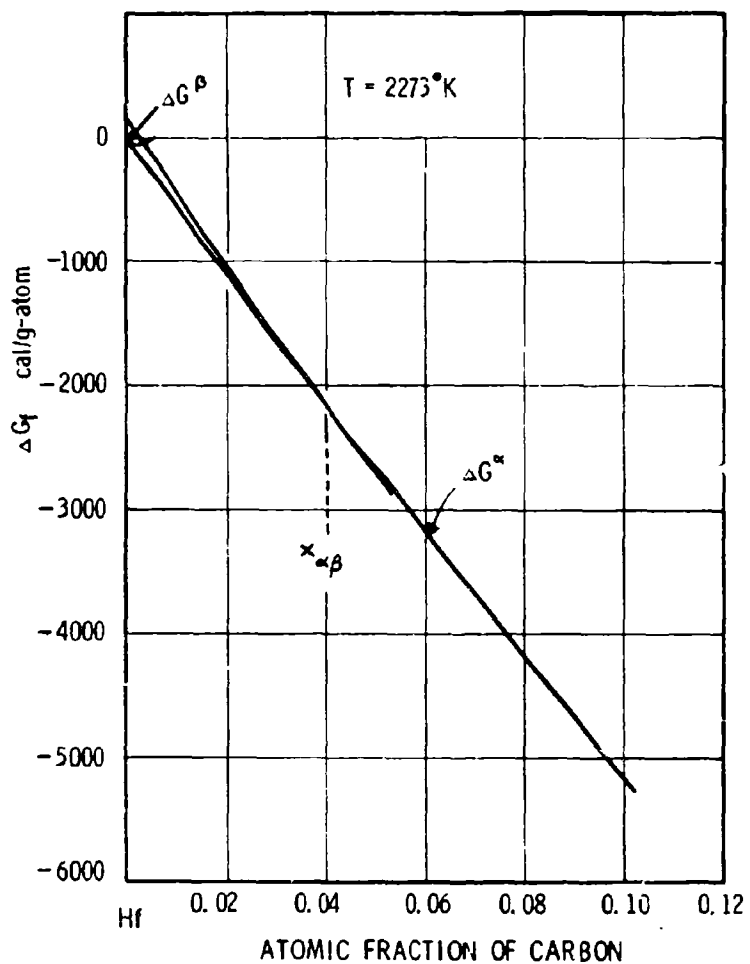


Figure 12b. Gibbs Free Energies of Formation of the α - and β -phases in the Hafnium-Carbon System

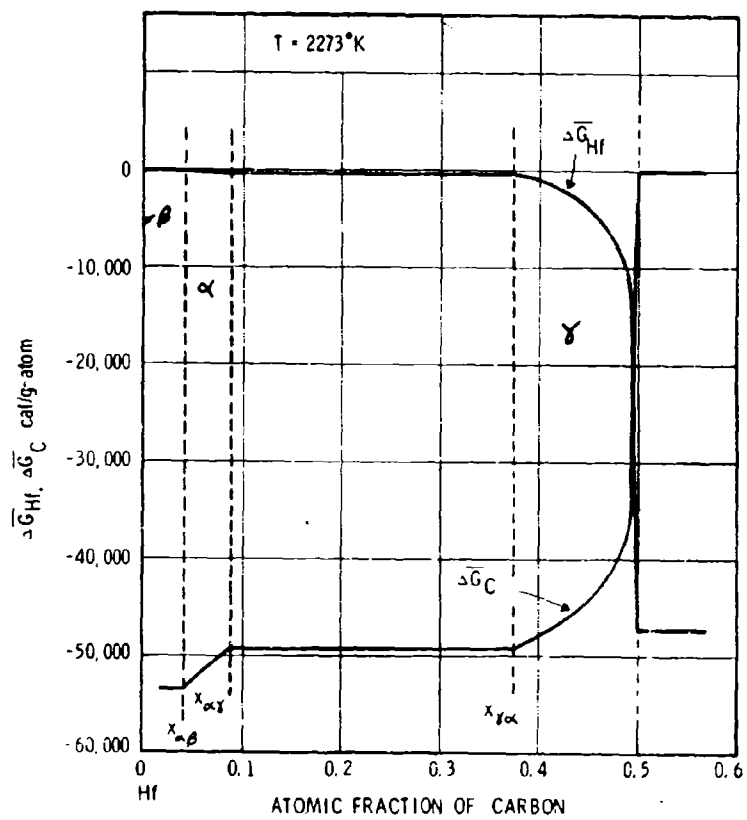


Figure 13. The Partial Molar Free Energies of Hafnium and Carbon

parameters, G_{Me+} , G_{C+} , and a for ZrC and TiC phases were calculated as a function of temperature.

We found that G_{Me+} and G_{C+} for both the ZrC and TiC phases decrease linearly with temperature, but a increases with temperature similar to the behavior of the three parameters for HfC phase. Again, the values of ΔG , $\Delta \bar{G}_{Me}$, and $\Delta \bar{G}_C$ for both the ZrC and TiC phases were calculated by means of an IBM-7094 computer as a function of temperature and composition based on the following three conditions:

$$a. \quad G_{C+} = 47,760 - 0.68 T \text{ for ZrC-phase} \quad (41)$$

$$G_{C+} = 45,600 - 2.93 T \text{ for TiC-phase} \quad (42)$$

$$b. \quad \Delta \bar{G}_{C, x=0.5} = 0 \quad (35a)$$

$$c. \quad \Delta \bar{G}_{Me, x=0.5} = 2\Delta G_{f, 0.5} \quad (35b)$$

The calculated integral and partial molar free energies for the ZrC phase at 2000°K and for the TiC phase at 1673°K are shown in Figures 14 through 17. At 2000°K, $G_{Zr+} = 88,740$, $G_{C+} = 46,400$, and $a = 0.4255 \times 10^{-5}$ for the ZrC phase. For the TiC phase, calculations at the temperature 1673°K gave the results: $G_{Ti+} = 78,940$, $G_{C+} = 40,700$, and $a = 0.2415 \times 10^{-5}$.

3. Discussion

The values of the vacancy parameter a for all the three group IV metal monocarbide phases: HfC, ZrC and TiC are small ($\sim 10^{-5}$) as calculated in the previous sections so that it was justified for us to use the approximate relationships to calculate the integral and partial molar free energies using the Schottky-Wagner vacancy model.

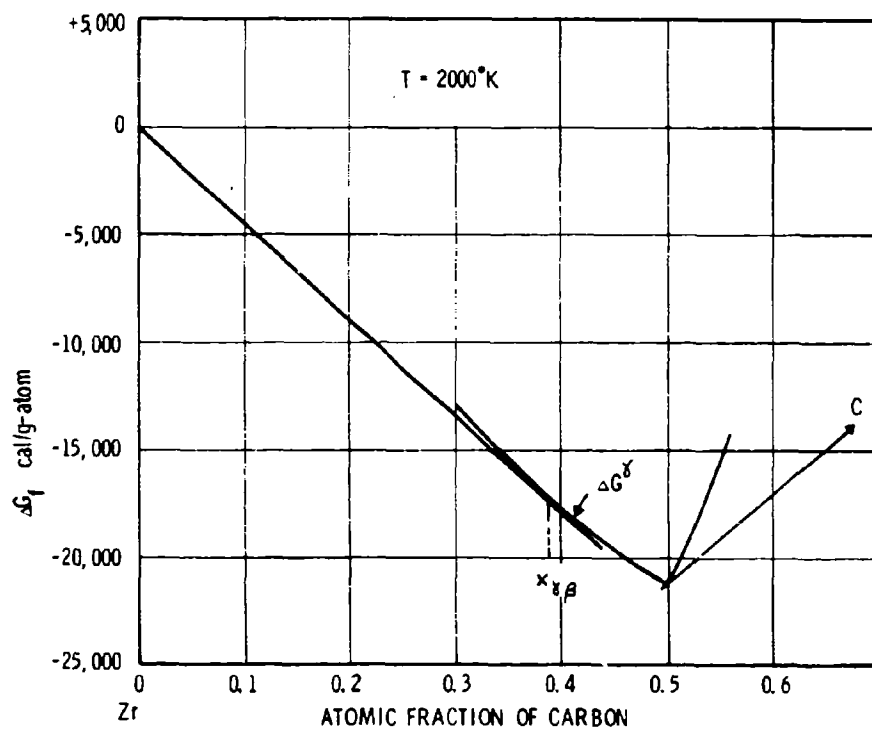


Figure 14. Gibbs Free Energy of Formation of the γ -phase in the Zirconium-Carbon System

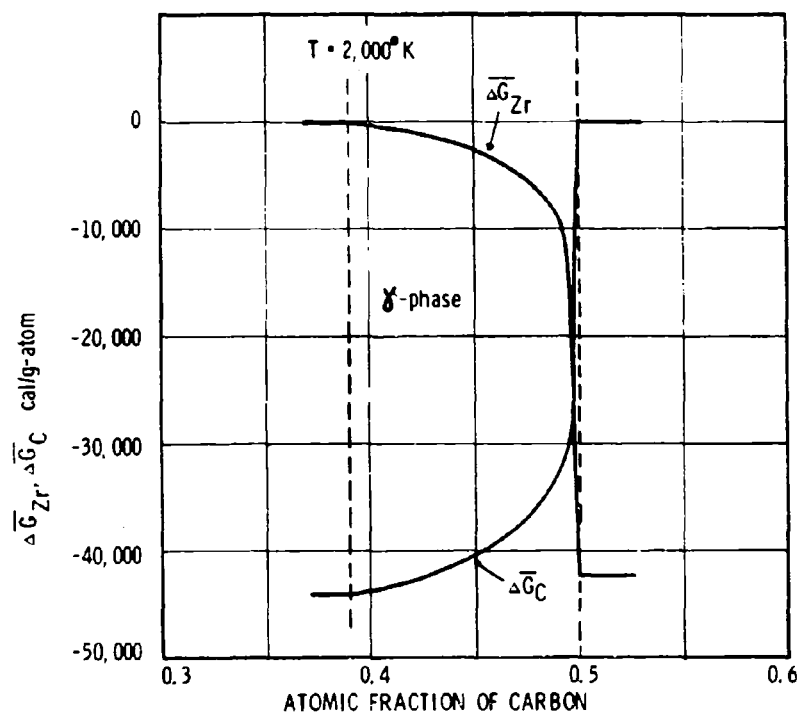


Figure 15. The Partial Molar Free Energies of Zirconium and Carbon

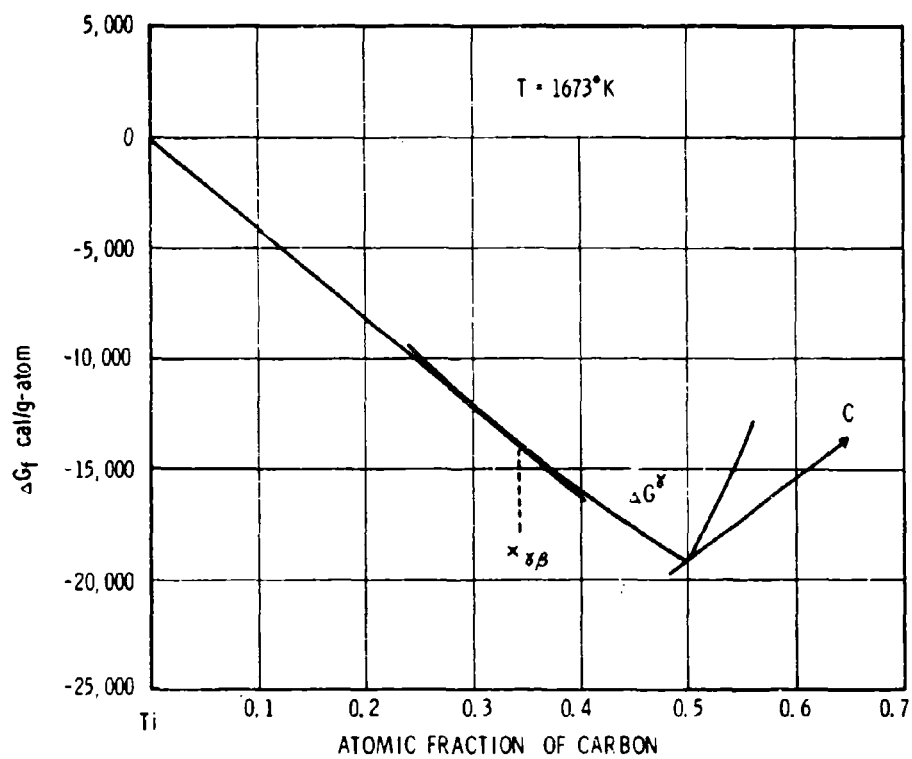


Figure 16. Gibbs Free Energy of Formation of the γ -phase in the Titanium-Carbon System

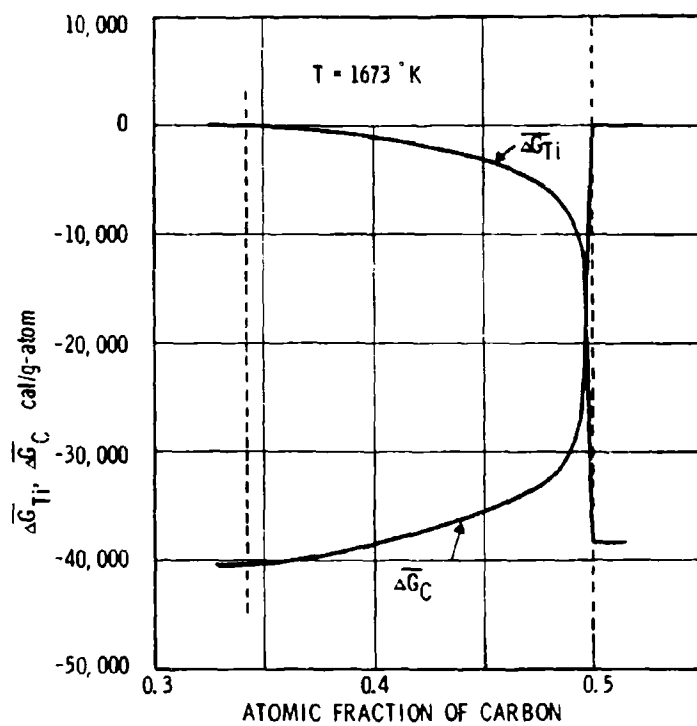


Figure 17. The Partial Molar Free Energies of Titanium and Carbon

The shapes of the integral free energy curves of the monocarbide phases as shown in Figures 12a, 14, and 16 are similar and are all typified by a sharp increase of the free energy at concentrations higher than the stoichiometric composition. This sharp rise of free energy is caused by the large free energies of creating metal vacancies on the metal sublattice.

At temperatures higher than the metal-rich eutectic temperature, the metal and carbon components at the metal-rich phase boundary of the monocarbide phase are no longer in equilibrium with the metal and carbon components in the terminal solid solution. Therefore, we do not now have the third boundary condition to evaluate all the three Schottky-Wagner parameters. However, since we have found that G_{C} decreases linearly with temperature at temperatures lower than the metal-rich eutectic temperature, we may assume that the linear relationship holds to even high temperatures. We can use this condition and the other two boundary conditions expressed by equations (35a) and (35b) to calculate the three parameters at any temperature. Once the values of the three parameters are known, one can calculate the integral and partial molar free energies as a function of composition.

Until experimental free energy data of the monocarbide phases as a function of composition and temperature becomes available, the calculated values using the Schottky-Wagner vacancy model are useful in calculating the phase diagrams of the ternary and higher order systems according to the method developed by Rudy⁽⁴⁷⁾ since we have chosen the three parameters such that the data are consistent with the binary phase diagrams.

REFERENCES

- (1) R. Hultgren, R.L. Orr, P.D. Anderson, and K.K. Kelley: "Selected Values of Thermodynamic Properties of Metals and Alloys", John Wiley and Sons, Inc., New York (1963)
- (2) E. Rudy: Private Communication
- (3) K.K. Kelley: Ind. Eng. Chem., 36, 865 (1944)
- (4) JANAF Thermochemical Tables, The Dow Chemical Company
- (5) B.F. Naylor: J. Am. Chem. Soc., 68, 370 (1946)
- (6) D.S. Neel: ASD-TR-62-765 (1963)
- (7) S.L. Bender, et.al.: ASD-TR-61-260, Part II, Vol.I (1962)
- (8) L.R. Brantley and A.O. Beckman: J.Am.Chem.Soc. 52, 3961 (1930)
- (9) J.F. Elliott and M. Gleiser: Thermochemistry for Steelmaking, Addison-Wesley Publishing Co., Inc. (1960)
- (10) V.S. Kutsev and B.F. Ormont: Zh.Flz. Khim., 31, 1866 (1957)
- (11) W.A. Chupka, J. Berkowitz, J. Giese, and M.G. Inghram: J. Phys. Chem. 62, 611 (1958)
- (12) S. Fujishiro and N.A. Gokcen: J. Phys. Chem., 65, 161 (1961)
- (13) J.A. Coffman, G.M. Kibler, T.F. Lyon, and B.P. Acchione: WADD-TR-60-646, Part II (1961)
- (14) A.S. Bolgar, T.S. Verkhoglyadova, and G.V. Samsonov: Otdel. Tekh. Nauk., Met.i.Izvest., Akad. Nauk. SSSR, Topliov 1961, 142 (1961)
- (15) E.K. Storms: LAMS-2674 (1962)
- (16) G.L. Humphrey: J. Am. Chem. Soc., 73, 2261 (1961)
- (17) C.E. Lowell and W.S. Williams: Rev.Sci.Instr., 32, 1120 (1961)
- (18) R.V. Sara, C.E. Lowell, and R.T. Dolloff: WADD-TR-60-143, Part IV (1963)

References (continued)

- (19) E.F. Westrum, Jr. and G. Felck: J. Chem. Engin. Data, 8, 176 (1963)
- (20) R. Mezaki, T.F. Jambois, A.K. Gangopadhyay, and J.L. Margrave: ASD-TDR-62-204, 92 (1963)
- (21) R.A. McDonald, F.L. Oetting, and H. Prophet: CPIA Publication No. 44 (u), (1964)
- (22) C.H. Prescott, Jr.: J. Am.Chem. Soc., 48, 2534 (1926)
- (23) V. Kutsev, B. Ormont, and V. Epelbaum: Doklady, Akad. Nauk., SSSR, 104, 567 (1955)
- (24) J.R. Hollahan and N.W. Gregory: J.Phys.Chem., 68, 2346 (1964)
- (25) B.P. Pollock: J. Phys.Chem., 65, 731 (1961)
- (26) A.D. Mah and B.J. Boyle: J.Am.Chem.Soc., 77, 6502 (1955)
- (27) A.D. Mah: U.S. Bureau of Mines RI 6518 (1964)
- (28) E.F. Westrum, Jr.: ASD-TDR-62, Part III, 193 (1964)
- (29) D.T. Hawkins, M. Onillon, and R.L. Orr: J.Chem.Engin. Data, 8, 628 (1963)
- (30) P. Blackburn, ASD-TDR-62, Part III, 98 (1964)
- (31) M.B. Panish and L. Reif: J.Chem.Phys., 38, 253 (1963)
- (32) G.M. Kibler, T.F. Lyon, M.J. Linevsky, and V.J. DeSantis: WADD-TR-60-646, Part IV, Volume II, 32 (1964)
- (33) L.S. Levinson: J. Chem.Phys., 40, 1437 (1964)
- (34) V.I. Zhelankin, V.S. Kutsev, and B.F. Ormont: Zh.Fiz.Khim. 33, 1988 (1959)
- (35) V.I. Zhelankin, V.S. Kutsev, and B.F. Ormont: Zh.Fiz.Khim. 35, 2608 (1961)
- (36) E. Rudy and H. Nowotny: Mona.Chem., 94, 507 (1963)
- (37) E.K. Storms and R.J. McNeal: J.Phys.Chem., 66, 1041 (1962)

References (continued)

- (38) C.H. Shomate and K.K. Kelley: J.Am.Chem.Soc., 71, 314 (1949)
- (39) Z. Bieganski and B. Stalinski: Bull.Acad.Polon.Sci. (Chim) 9, 367 (1961)
- (40) E.G. King: J. Am.Chem.Soc., 71, 316 (1949)
- (41) W.L. Worrell and J. Chipman: J.Phys.Chem., 60, 860 (1964)
- (42) V.I. Alekseev and L.A. Shvartsman: Doklady, Akad.Nauk,SSSR, 113, 1331 (1960)
- (43) V.K. Alekseev and L.A. Shvartsman: Fiz.Metal.Metalloved, 11, 545 (1961)
- (44) F.D. Richardson: J.Iron Steel Inst., 175, 33 (1953)
- (45) G.Brauer and W.D. Schnell: J. Less-Common Metals, 7, 23-30 (1964)
- (46) H. Krainer and K. Konopicky: Berg-Heuttenmaenn. Monatsh. Montan. Hochschule, Leoben, 92, 166 (1947)
- (47) E. Rudy: Z. Metallk., 54, 213 (1963)
- (48) S. Fujishiro and N.A. Gokcen: J. Electrochem.Soc., 109, 835 (1962)
- (49) A.D. Mah: U.S. Bureau of Mines RI 6177 (1963)
- (50) K.K. Kelley: U.S. Bureau of Mines, Bulletin 584, Contribution to the data on Theoretical Metallurgy, XIII, (1960)
- (51) E.K. Storms and N.H. Krikorian: J.Phys.Chem., 64, 1471 (1960)
- (52) L.B. Pankratz, W.W. Weller, and K.K. Kelley: U.S. Bureau of Mines RI 6446 (1964)
- (53) P.V. Gel'd and F.G. Kussenko: Izvest.Akad. Nauk.SSSR., Otd. Teckhn. Nauk. Met. i Topliov, 79-86 (1960)
- (54) L.S. Levinson: J.Chem. Phys., 39, 1550 (1963)
- (55) W.L. Worrell: J. Phys.Chem. 68, 952 (1964)
- (56) R.J. Fries: J. Chem.Phys., 37, 320 (1962)

References (continued)

- (57) E.J. Huber, Jr., E.L. Head, C.E. Holley, Jr., E.K. Storms, and N.H. Krikorian: J. Phys.Chem., 65, 1846 (1957)
- (58) A.N. Kornikov, V. Ya. Leonidov, and S.M. Skuratov: Abstract of J. Phys. Metallurgy, Vestn.Mosk. Univ.Ser.Khim. No. 6, p 48 (1962)
- (59) F.G. Kussenko and P.V. Gel'd: Izvest.Sibir.Otdel.Akad. Nauk. SSSR, 2, 46 (1960)
- (60) E. Rudy, C. Brukl, and D.P. Harmon: Private Communication
- (61) K.K. Kelley: J. Am.Chem.Soc., 62, 818 (1940)
- (62) K.K. Kelley and E.G. King: U.S. Bureau of Mines Bulletin, 592, XIV. Entropies of the Elements and Inorganic Compounds (1961)
- (63) G.L. Humphrey: J.Am.Chem. Soc., 76, 978 (1954)
- (64) M. Hoch, P.E. Blackburn, D.P. Dingley, and H.L. Johnston: J. Phys. Chem., 59, 97 (1955)
- (65) A.D. Mah, Private Communication from E.G. King: U.S. Bureau of Mines, Berkeley, California
- (66) E.J. Huber, Jr., E.L. Head, C.E. Holley, Jr., and A.L. Bowman: J.Phys. Chem. 67, 793 (1963)
- (67) V.I. Smirnova and B.F. Ormont: Dokl.Akad. Nauk. SSSR, 100, 127 (1955), Zh. Fiz. Khim. 30, 1327 (1956)
- (68) D.S. Bloom, N.J. Grant: Trans. AIME, 188, 41 (1950)
- (69) K.K. Kelley, F.S. Boericke, G.E. Moore, E.H. Huffman, and W.M. Bangert: U.S. Bureau of Mines Tech.Paper 662 (1944)
- (70) W. L. Sorbo : J. Am.Chem. Soc., 75, 1825 (1953)
- (71) R.A. Oriani and W.K. Murphy: J.Am.Chem.Soc., 76, 343 (1954)
- (72) A.D. Mah: J. Am. Chem.Soc., 76, 3363 (1954)
- (73) M. Gleiser: to be published in J. Phys. Chem., private communication from Dr. W.L. Worrell, Lawrence Radiation Laboratory, Berkeley, California.

References (continued)

- (74) E. Rudy and Y.A. Chang: Plansee Proceedings 1964, Edited by F. Benesovsky, Metallwerk Plansee, AG., Reutte, Tirol, 786 (1965)
- (75) S. Fujishiro and N.A. Gokcen: Trans. AIME, 221, 275 (1961)
- (76) F.Z. Vintaikin: Fiz.Metall.Metalloved., 15, 144 (1963)
- (77) E. Rudy, S. Windisch, and Y.A. Chang: AFML-TR-65-2, Part I, Vol. I. (1965)
- (78) E. Parthé and V. Sadagopan: Mh.Chem., 93, 263 (1962)
- (79) O.H. Krikorian: UCRL-6785 (1962)
- (80) M. Gleiser and J. Chipman: J.Phys.Chem., 66, 1539 (1962)
- (81) R. Schenck, F. Kurzen, and H. Wesselkock: Z. anorg. allgen. Chem., 203, 159 (1932)
- (82) A.D. Mah: U.S. Bureau of Mines RI 6337 (1963)
- (83) E. Rudy and S. Windisch: AFML-TR-65-2, Part I, Vol.II. (1965)
- (84) M. Gleiser and J. Chipman: Trans. AIME, 224, 1278-9 (1962)
- (85) V.I. Alekseev and L.A. Shvartsman: Izvest.Akad.Nauk.SSSR, Met. i. Gornoe. Delo, 9196 (1963)
- (86) G.W. Orton: Ph.D. Thesis, Ohio State University (1961)
- (87) L.D. McGraw, H. Seltz, and P. Snyder: J. Am.Chem.Soc., 69, 329 (1947)
- (88) A.D. Mah: J.Am.Chem.Soc., 81, 1582 (1959)
- (89) W. Schottky and C. Wagner: Z. Physik.Chem., 11, 163 (1931)
- (90) C. Wagner: Thermodynamics of Alloys, Addison-Wesley, Reeding, Mass. (1952)
- (91) L. Kaufman, H. Bernstein, and A. Sarney: ASD-TR-6-445, Part IV, (1963)

| DOCUMENT CONTROL DATA - R&D | | |
|--|---|--|
| (Security classification of title, body of abstract and indexing annotation must be entered when the overall report is classified) | | |
| 1. ORIGINATING ACTIVITY (Corporate author) | | 2a. REPORT SECURITY CLASSIFICATION |
| Materials Research Laboratory Aerojet-General Corporation Sacramento, California | | Unclassified |
| | | 2b. GROUP |
| | | N.A. |
| 3. REPORT TITLE | | |
| Ternary Phase Equilibria in Transition Metal-Boron-Carbon-Silicon Systems. Part IV. Thermochemical Calculations Vol. I. Thermodynamic Properties of Group IV, V, and VI Binary Transition Metal Carbides | | |
| 4. DESCRIPTIVE NOTES (Type of report and inclusive dates) | | |
| 5. AUTHOR (Last name, first name, initial) | | |
| Y. Austin Chang | | |
| 6. REPORT DATE | 7a. TOTAL NO. OF PAGES | 7b. NO. OF REFS |
| 11 June 1965 | 103 | 91 |
| 8a. CONTRACT OR GRANT NO. | 9a. ORIGINATOR'S REPORT NUMBER(S) | |
| AF 33(615)-1249 | AFML TR-65-2-11-1-1 | |
| 8b. PROJECT NO. | 9b. OTHER REPORT NO(S) (Any other numbers that may be assigned this report) | |
| 7350 | N.A. | |
| 8c. Task No. | | |
| 735001 | | |
| 10. AVAILABILITY/LIMITATION NOTICES | | |
| Qualified requesters may obtain copies of this report from DDC | | |
| 11. SUPPLEMENTARY NOTES | | 12. SPONSORING MILITARY ACTIVITY |
| | | AFML (MAMC) Wright-Patterson AFB, Ohio, 45433 |
| 13. ABSTRACT | | |
| <p>All available data concerning the thermodynamic properties of the group IV, V, and VI binary metal carbides have been critically evaluated and the values judged to be most reliable were selected. The compositional variation of the free energies of the group IV binary metal carbides has been calculated based on theoretical models.</p> | | |

DD FORM 1473
1 JAN 64

Unclassified

Security Classification

Unclassified

Security Classification

FORM 107-1 (1-77) (M) (U)

| 14. KEY WORDS | LINK A | | LINK B | | LINK C | |
|--|--------|----|--------|----|--------|----|
| | ROLE | WT | ROLE | WT | ROLE | WT |
| Thermodynamic Properties Carbides Phase Diagrams | | | | | | |

INSTRUCTIONS

1. **ORIGINATING ACTIVITY:** Enter the name and address of the contractor, subcontractor, grantee, Department of Defense activity or other organization (corporate author) issuing the report.

2a. **REPORT SECURITY CLASSIFICATION:** Enter the overall security classification of the report. Indicate whether "Restricted Data" is included. Marking is to be in accordance with appropriate security regulations.

2b. **GROUP:** Automatic downgrading is specified in DoD Directive 5200.10 and Armed Forces Industrial Manual. Enter the group number. Also, when applicable, show that optional markings have been used for Group 3 and Group 4 as authorized.

3. **REPORT TITLE:** Enter the complete report title in all capital letters. Titles in all cases should be unclassified. If a meaningful title cannot be selected without classification, show title classification in all capitals in parenthesis immediately following the title.

4. **DESCRIPTIVE NOTES:** If appropriate, enter the type of report, e.g., interim, progress, summary, annual, or final. Give the inclusive dates when a specific reporting period is covered.

5. **AUTHOR(S):** Enter the name(s) of author(s) as shown on or in the report. Enter last name, first name, middle initial. If military, show rank and branch of service. The name of the principal author is an absolute minimum requirement.

6. **REPORT DATE:** Enter the date of the report as day, month, year, or month, year. If more than one date appears on the report, use date of publication.

7a. **TOTAL NUMBER OF PAGES:** The total page count should follow normal pagination procedures. I.e., enter the number of pages containing information.

7b. **NUMBER OF REFERENCES:** Enter the total number of references cited in the report.

8a. **CONTRACT OR GRANT NUMBER:** If appropriate, enter the applicable number of the contract or grant under which the report was written.

8b, &c, & 8d. **PROJECT NUMBER:** Enter the appropriate military department identification, such as project number, subproject number, system numbers, task number, etc.

9a. **ORIGINATOR'S REPORT NUMBER(S):** Enter the official report number by which the document will be identified and controlled by the originating activity. This number must be unique to this report.

9b. **OTHER REPORT NUMBER(S):** If the report has been assigned any other report numbers (either by the originator or by the sponsor), also enter this number(s).

10. **AVAILABILITY/LIMITATION NOTICES:** Enter any limitations on further dissemination of the report, other than those

imposed by security classification, using standard statements such as:

- (1) "Qualified requesters may obtain copies of this report from DDC."
- (2) "Foreign announcement and dissemination of this report by DDC is not authorized."
- (3) "U. S. Government agencies may obtain copies of this report directly from DDC. Other qualified DDC users shall request through _____."
- (4) "U. S. military agencies may obtain copies of this report directly from DDC. Other qualified users shall request through _____."
- (5) "All distribution of this report is controlled. Qualified DDC users shall request through _____."

If the report has been furnished to the Office of Technical Services, Department of Commerce, for sale to the public, indicate this fact and enter the price, if known.

11. **SUPPLEMENTARY NOTES:** Use for additional explanatory notes.

12. **SPONSORING MILITARY ACTIVITY:** Enter the name of the departmental project office or laboratory sponsoring (paying for) the research and development. Include address.

13. **ABSTRACT:** Enter an abstract giving a brief and factual summary of the document indicative of the report, even though it may also appear elsewhere in the body of the technical report. If additional space is required, a continuation sheet shall be attached.

It is highly desirable that the abstract of classified reports be unclassified. Each paragraph of the abstract shall end with an indication of the military security classification of the information in the paragraph, represented as (TS), (S), (C), or (U).

There is no limitation on the length of the abstract. However, the suggested length is from 150 to 225 words.

14. **KEY WORDS:** Key words are technically meaningful terms or short phrases that characterize a report and may be used as index entries for cataloging the report. Key words must be selected so that no security classification is required. Identifiers, such as equipment model designation, trade name, military project code name, geographic location, may be used as key words but will be followed by an indication of technical context. The assignment of links, rules, and weights is optional.

Unclassified

Security Classification